Journal of Scientific Computing (2022) 93:75
https://doi.org/10.1007/s10915-022-02035-y

An Unfitted Finite Element Method by Direct Extension for Elliptic Problems on Domains with Curved Boundaries and Interfaces

Fanyi Yang[1] · **Xiaoping Xie**[1]

Received: 19 March 2022 / Revised: 15 October 2022 / Accepted: 16 October 2022 /
Published online: 5 November 2022

Abstract
We propose and analyze an unfitted finite element method of arbitrary order for solving elliptic problems on domains with curved boundaries and interfaces. The approximation space on the whole domain is obtained by the direct extension of the finite element space defined on interior elements, in the sense that there is no degree of freedom locating in boundary/interface elements. We apply a non-symmetric bilinear form and the boundary/jump conditions are imposed in a weak sense in the scheme. The method is shown to be stable without any mesh adjustment or any special stabilization. The optimal convergence rate under the energy norm is derived, and $O(h^{-2})$-upper bounds of the condition numbers are shown for the final linear systems. Numerical results in both two and three dimensions are presented to illustrate the accuracy and the robustness of the method.

Keywords Elliptic problems · Curved boundary · Interface problems · Finite element method · Nitsche's method · Unfitted mesh

1 Introduction

In recent two decades, unfitted finite element methods have become widely used tools in the numerical analysis of problems with interfaces and complex geometries [4, 6, 7, 18, 20, 26, 33, 36, 37, 39, 40, 45]. For such kinds of problems, the generation of the body-fitted meshes is usually a very challenging and time-consuming task, especially in three dimensions. The unfitted methods avoid the task to generate high quality meshes for representing the domain geometries accurately, due to the use of meshes independent of the interfaces and domain boundaries and the use of certain enrichment of finite element basis functions characterizing the solution singularities or discontinuities.

✉ Xiaoping Xie
xpxie@scu.edu.cn

Fanyi Yang
yangfanyi@scu.edu.cn

[1] School of Mathematics, Sichuan University, Chengdu 610064, China

In [26], Hansbo and Hansbo proposed an unfitted finite element method for elliptic interface problems. The numerical solution comes from two separate linear finite element spaces and the jump conditions are weakly enforced by Nitsche's method. This idea has been a popular discretization for interface problems and has also been applied to many other interface problems, see [12, 13, 28] and the references therein for further advances. This method can also be written into the framework of extended finite element method by a Heaviside enrichment [2, 6, 18]. We note that for penalty methods, the small cuts of the mesh have to be treated carefully, which may adversely effect the conditioning of the method and even hamper the convergence [10, 16]. In [30], Johansson and Larson proposed an unfitted high-order discontinuous Galerkin method on structured grids, where they constructed large extended elements to cure the issue of the small cuts and obtain the stability near the interface. Similar ideas of merging elements for interface problems can also be found in [10, 29, 38]. Another popular unfitted method is the cut finite element method [11], which is a variation of the extended finite element method. This method involves the ghost penalty technique [9] to guarantee the stability of the scheme. In addition, Massing and Gürkan developed a framework combining the cut finite element method and the discontinuous Galerkin method [20]. We refer to [7, 11, 14, 22, 25, 42] and the references therein for some recent applications of the cut finite element method. Badia et al. proposed an aggregated unfitted finite element method for elliptic problems [5, 43]. The main idea of this method is to construct the enhanced finite element spaces based on a cell aggregation strategy to address the small cut problem. Kramer et al. [33] presented a new extended finite element method with the algebraic constants on cut elements to enforce the continuity condition. In [35], Lehrenfeld introduced a high order unfitted finite element method based on isoparametric mappings, where the piecewise interface is mapped approximately onto the zero level set of a high-order approximation of the level set function. We refer to [36] for a detailed analysis of this method. Main and Scovazzi [41] and Li et al. [37] proposed the shifted boundary/interface method. The main idea of this approach is to shift the location of boundary/interface to the surrogate domain.

In this article, we propose a new unfitted finite element method for second order elliptic problems on domains with curved boundaries and interfaces. The novelty of this method lies in that the approximation space is obtained by the direct extension of a common finite element space. We first define a standard finite element space on the set of all interior elements which are not cut by the domain boundary/interface. Then an extension operator is introduced for this space. This operator defines the polynomials on cut elements by directly extending the polynomials defined on some interior neighbouring elements. Then the approximation space is obtained from the extension operator. In the discrete schemes, a non-symmetric interior penalty method is proposed, and the boundary/jump conditions on the interface are satisfied in a weak sense. We derive optimal error estimates under the energy norm, and we give upper bounds of the condition numbers of the final linear systems. The curved boundary/interface is allowed to intersect the mesh arbitrarily in our method. We note that the idea of constructing discrete extension operators can also be found in [5, 10]. This kind of methods define conforming finite element spaces from interior nodal values with the help of the extension operators. Different from [5, 10], in our method, the polynomials defined on cut elements are just the same polynomials on the assigned interior neighbouring elements, and there is no need to compute the nodal values and corresponding basis functions on cut elements. The implementation of the proposed method is simple and straightforward. We also note that although our approximation space is not conforming, the resultant scheme only requires a parameter-friendly penalty term defined on the boundary/interface. We conduct a series of numerical experiments in two and three dimensions to illustrate the convergence

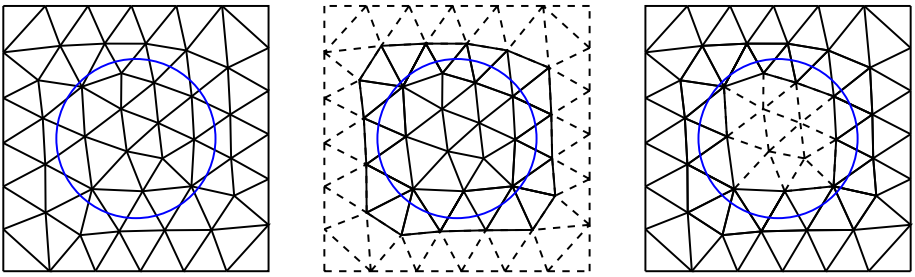

Fig. 1 The background mesh $\mathcal{T}_h$ (left) / the mesh $\mathcal{T}_{h,0}$ (mid) /the mesh $\mathcal{T}_{h,1}$ (right)

behaviour. The numerical solution shows the optimal convergence rates for both the energy norm and the L^2 norm.

The rest of this article is organized as follows. In Sect. 2, we introduce notations and prove some basic properties for the approximation space. We show the unfitted finite element method for the elliptic problem on a curved domain and the elliptic interface problem in Sects. 3 and 4, respectively, and we derive the error estimates, and give upper bounds of the condition numbers of the discrete systems. In Sect. 5, we perform some numerical tests to confirm the optimal convergence rates and show the robustness of the proposed method. Finally, we make a conclusion in Sect. 6.

2 Preliminaries

Let $\Omega \subset \mathbb{R}^d (d = 2, 3)$ be a convex polygonal (polyhedral) domain with boundary $\partial\Omega$. Let $\Omega_0 \Subset \Omega$ be an open subdomain with C^2-smooth or convex polygonal (polyhedral) boundary. We denote by $\Gamma := \partial\Omega_0$ the topological boundary. We define $\Omega_1 := \Omega \backslash \overline{\Omega}_0$, and clearly there holds $\overline{\Omega}_0 \cup \overline{\Omega}_1 = \overline{\Omega}$ and $\Omega_0 \cap \Omega_1 = \varnothing$. Let $\mathcal{T}_h$ be a background mesh, which is a quasi-uniform and regular triangulation of the domain Ω into open simplexes (see Fig. 1 for the example that Γ is a circle). We denote by $\mathcal{E}_h$ the collection of all $d-1$ dimensional faces in $\mathcal{T}_h$, and $\mathcal{E}_h$ is further decomposed into $\mathcal{E}_h = \mathcal{E}_h^B \cup \mathcal{E}_h^I$, where $\mathcal{E}_h^B$ and $\mathcal{E}_h^I$ consist of boundary faces and interior faces, respectively. For any element $K \in \mathcal{T}_h$ and any face $e \in \mathcal{E}_h$, we denote by h_K and h_e their diameters, respectively. The mesh size h is defined as $h := \max_{K\in\mathcal{T}_h} h_K$. The quasi-uniformity of $\mathcal{T}_h$ is in the sense of that there exists a constant C such that $h \le C\rho_K$ for any element K,there exists a constant ν such that $h \le \nu \min_{K\in\mathcal{T}_h} \rho_K$, where ρ_K is the radius of the largest ball inscribed in K.

Remark 1 The assumed quasi-uniformity of $\mathcal{T}_h$ is mostly for the convenience of notations. Most estimates in this paper only require the shape-regularity of the partition, except for the estimate of the condition number.

For $i = 0, 1$, we set

$$\mathcal{T}_{h,i} := \{K \in \mathcal{T}_h \mid K \cap \Omega_i \neq \varnothing\}, \quad \mathcal{T}_{h,i}^\circ := \{K \in \mathcal{T}_{h,0} \mid K \subset \Omega_i\},$$

where $\mathcal{T}_{h,i}$ is the minimal subset of $\mathcal{T}_h$ that just covers the domain $\overline{\Omega}_i$, and $\mathcal{T}_{h,i}^\circ$ is the set of elements which are inside the domain Ω_i. We define the corresponding domains $\Omega_{h,i} := \mathrm{Int}(\bigcup_{K\in\mathcal{T}_{h,i}} \overline{K})$ and $\Omega_{h,i}^\circ := \mathrm{Int}(\bigcup_{K\in\mathcal{T}_{h,i}^\circ} \overline{K})$. Clearly, there holds $\Omega_{h,i}^\circ \subset \Omega_i \subset \Omega_{h,i}$. We define $\mathcal{E}_{h,i}$ and $\mathcal{E}_{h,i}^\circ$ as the collections of $d-1$ dimensional faces for the partitions $\mathcal{T}_{h,i}$ and $\mathcal{T}_{h,i}^\circ$,

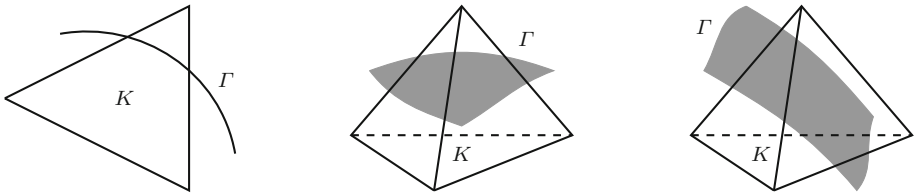

Fig. 2 Examples of cut elements in two and three dimensions

respectively. Further, $\mathcal{E}_{h,i}$ is decomposed into $\mathcal{E}_{h,i} = \mathcal{E}_{h,i}^I \cup \mathcal{E}_{h,i}^B$, where $\mathcal{E}_{h,i}^I$ and $\mathcal{E}_{h,i}^B$ consist of interior faces and boundary faces in $\mathcal{T}_{h,i}$, respectively. Similarly, $\mathcal{E}_{h,i}^\circ$ is decomposed into $\mathcal{E}_{h,i}^\circ = \mathcal{E}_{h,i}^{\circ,I} \cup \mathcal{E}_{h,i}^{\circ,B}$, where $\mathcal{E}_{h,i}^{\circ,I}$ and $\mathcal{E}_{h,i}^{\circ,B}$ are sets of interior faces and boundary faces in $\mathcal{T}_{h,i}^\circ$, respectively. We denote by $\mathcal{T}_h^\Gamma$ and $\mathcal{E}_h^\Gamma$ the sets of elements and faces that are cut by Γ, respectively:

$$\mathcal{T}_h^\Gamma := \{K \in \mathcal{T}_h \mid K \cap \Gamma \neq \varnothing\}, \quad \mathcal{E}_h^\Gamma := \{e \in \mathcal{E}_h \mid e \cap \Gamma \neq \varnothing\}.$$

Obviously, there holds $\mathcal{T}_h^\Gamma = \mathcal{T}_{h,i} \backslash \mathcal{T}_{h,i}^\circ (i = 0, 1)$ and $\mathcal{E}_h^\Gamma = \mathcal{E}_{h,i}^I \backslash \mathcal{E}_{h,i}^\circ (i = 0, 1)$. For any element $K \in \mathcal{T}_h^\Gamma$, we define

$$\Gamma_K := K \cap \Gamma, \quad (\partial K)^0 := (\partial K \cap \Omega_0) \cup \Gamma_K, \quad (\partial K)^1 := (\partial K \cap \Omega_1) \cup \Gamma_K. \tag{1}$$

For any element $K \in \mathcal{T}_h$ and any face $e \in \mathcal{E}_h$, we define

$$K^0 := K \cap \Omega_0, \quad K^1 := K \cap \Omega_1, \quad e^0 := e \cap \overline{\Omega}_0, \quad e^1 := e \cap \overline{\Omega}_1. \tag{2}$$

We make following natural geometrical assumptions on the background mesh:

Assumption 1 For any cut face $e \in \mathcal{E}_h^\Gamma$, the intersection $e \cap \Gamma$ is simply connected; that is, Γ does not cross a face multiple times (cf. Figure 2).

Assumption 2 For any cut element $K \in \mathcal{T}_h^\Gamma$, Γ cross at least d faces of K.

Assumption 3 For any cut element $K \in \mathcal{T}_h^\Gamma$, there exist two elements $K_0^\circ \in \Delta(K) \cap \mathcal{T}_{h,0}^\circ$, $K_1^\circ \in \Delta(K) \cap \mathcal{T}_{h,1}^\circ$, where $\Delta(K) := \{K' \in \mathcal{T}_h \mid \overline{K'} \cap \overline{K} \neq \varnothing\}$ denotes the set of elements that touch K.

Assumption 4 For any face $e \in \mathcal{E}_h^\Gamma$ with $e = \partial\widehat{K} \cap \partial\widetilde{K}$, we assume that there exists a constant L such that the assigned element $(\widehat{K})_0^\circ \in \mathcal{T}_{h,0}^\circ$ can be reached from the assigned element $(\widetilde{K})_0^\circ \in \mathcal{T}_{h,0}^\circ$ by crossing at most L interior elements; that is there exist a sequence of elements $K_0, K_1, \ldots, K_M (M \leq L)$ such that $K_0 = (\widehat{K})_0^\circ$, $K_M = (\widetilde{K})_0^\circ$, $K_i \in \mathcal{T}_{h,0}^\circ$ and K_i is adjacent to K_{i+1} for $1 \leq i \leq M - 1$. We also assume that the element $(\widehat{K})_1^\circ \in \mathcal{T}_{h,1}^\circ$ can be reached from the element $(\widetilde{K})_1^\circ \in \mathcal{T}_{h,1}^\circ$ by crossing at most L interior elements in the same sense.

Remark 2 The above assumptions are widely used in interface problems [23, 27, 47], which ensure the curved boundary Γ is well-resolved by the mesh. We note that if the mesh is fine enough, Assumptions 1 - 4 can always be fulfilled.

Here we give the method for selecting the elements K_0° and K_1° for any cut element K. For any $K \in \mathcal{T}_h^\Gamma$, we define $N(K) := \{K' \in \mathcal{T}_h \mid \partial K' \cap \partial K = e \in \mathcal{E}_h\}$ as the set of all face-neighbouring elements of K. We note that $N(K) \cap \mathcal{T}_{h,0}^\circ$ has at most one element from the above assumptions. If $N(K) \cap \mathcal{T}_{h,0}^\circ$ is not empty, choose the element in $N(K) \cap \mathcal{T}_{h,0}^\circ$ as K_0°; otherwise pick an arbitrary element in $\Delta(K) \cap \mathcal{T}_{h,0}^\circ$ as K_0°. Generally, we choose K_0° sharing a face with K whenever possible in the computer implementation. The element K_1° is selected in the same way.

From the quasi-uniformity of the mesh, there exists a constant C_Δ independent of h such that for any element $K \in \mathcal{T}_h$, there is a ball $B(\boldsymbol{x}_K, C_\Delta h_K)$ satisfying $\Delta(K) \subset B(\boldsymbol{x}_K, C_\Delta h_K)$, where $\boldsymbol{x}_K$ is the barycenter of K and $B(\boldsymbol{z}, r)$ denotes the ball centered at $\boldsymbol{z}$ with radius r. Moreover, let Ω^* be an open bounded domain, independent of the mesh size h and Γ, which includes the union of all balls $B(\boldsymbol{x}_K, C_\Delta h_K)$ ($\forall K \in \mathcal{T}_h$), that is, $B(\boldsymbol{x}_K, C_\Delta h_K) \subset \Omega^*$ for any $K \in \mathcal{T}_h$.

Next, we introduce the jump and average operators which are widely used in the discontinuous Galerkin framework. Let $e \in \mathcal{E}_h^I$ be any interior face shared by two neighbouring elements K^+ and K^-, with the unit outward normal vectors $\mathbf{n}^+$ and $\mathbf{n}^-$ along e, respectively. For any piecewise smooth scalar-valued function v and piecewise smooth vector-valued function $\boldsymbol{q}$, the jump operator $[\![\cdot]\!]$ is defined as

$$[\![v]\!]|_e := v^+|_e \mathbf{n}^+ + v^-|_e \mathbf{n}^-, \quad [\![\boldsymbol{q}]\!]|_e := \boldsymbol{q}^+|_e \cdot \mathbf{n}^+ + \boldsymbol{q}^-|_e \cdot \mathbf{n}^-,$$

where $v^+ := v|_{K^+}$, $v^- := v|_{K^-}$, $\boldsymbol{q}^+ := \boldsymbol{q}|_{K^+}$, $\boldsymbol{q}^- := \boldsymbol{q}|_{K^-}$, and the average operator $\{\cdot\}$ is defined as

$$\{v\}|_e := \frac{1}{2}\left(v^+|_e + v^-|_e\right), \quad \{\boldsymbol{q}\}|_e := \frac{1}{2}\left(\boldsymbol{q}^+|_e + \boldsymbol{q}^-|_e\right).$$

On a boundary face $e \in \mathcal{E}_h^B$ with the unit outward normal vector $\mathbf{n}$, we define

$$\{v\}|_e := v|_e, \quad [\![v]\!]|_e := v|_e \mathbf{n}, \quad \{\boldsymbol{q}\}|_e := \boldsymbol{q}|_e, \quad [\![\boldsymbol{q}]\!]|_e := \boldsymbol{q}|_e \cdot \mathbf{n}.$$

We will also employ the jump operator $[\![\cdot]\!]$ and the average $\{\cdot\}$ on Γ, that is,

$$[\![v]\!]|_\Gamma, \quad \{v\}|_\Gamma, \quad [\![\boldsymbol{q}]\!]|_\Gamma, \quad \{\boldsymbol{q}\}|_\Gamma, \tag{3}$$

and their definitions will be given later for specific problems.

For a bounded domain D, we follow the standard notations of the Sobolev spaces $L^2(D)$, $H^r(D)(r \geq 0)$ and their corresponding inner products, norms and semi-norms. For the partition $\mathcal{T}_h$, the notations of broken Sobolev spaces $L^2(\mathcal{T}_h)$, $H^r(\mathcal{T}_h)$ are also used as well as their associated inner products and broken Sobolev norms.

Throughout this paper, we denote by C and C with subscripts the generic positive constants that may vary between lines but are independent of the mesh size h and how Γ cuts the mesh $\mathcal{T}_h$.

For $i = 0, 1$, we follow three steps to give the definition of the approximation space $V_{h,i}^m$ with respect to the partition $\mathcal{T}_{h,i}$.

Step 1. Let $V_{h,i}^{m,\circ}$ be the space of piecewise polynomials of degree $m \geq 1$ on $\mathcal{T}_{h,i}^\circ$. Here $V_{h,i}^{m,\circ}$ can be a standard C^0 finite element space or a discontinuous finite element space, i.e.

$$V_{h,i}^{m,\circ} = \{v_h \in C(\Omega_{h,i}^\circ) \mid v_h|_K \in \mathbb{P}_m(K),\ \forall K \in \mathcal{T}_{h,i}^\circ\},$$

or

$$V_{h,i}^{m,\circ} = \{v_h \in L^2(\Omega_{h,i}^\circ) \mid v_h|_K \in \mathbb{P}_m(K),\ \forall K \in \mathcal{T}_{h,i}^\circ\},$$

where $\mathbb{P}_m(K)$ denotes the set of polynomials of degree m defined on K.

Step 2. We extend the space $V_{h,i}^{m,\circ}$ to the mesh $\mathcal{T}_{h,i}$ by introducing an extension operator $E_{h,i}$. To this end, for every element $K \in \mathcal{T}_h$, we define a local extension operator

$$\begin{aligned} E_K : \mathbb{P}_m(K) &\to \mathbb{P}_m(B(\boldsymbol{x}_K, C_\Delta h_K)), \\ v &\mapsto E_K v, \end{aligned} \qquad v|_K = (E_K v)|_K. \tag{4}$$

For any $v \in \mathbb{P}_m(K)$, $E_K v$ is a polynomial defined on the ball $B(\boldsymbol{x}_K, C_\Delta h_K)$ and has the same expression as v. Then the operator $E_{h,i}$ is defined in a piecewise manner: for any $K \in \mathcal{T}_{h,i}$ and $v_h \in V_{h,i}^{m,\circ}$,

$$(E_{h,i} v_h)|_K := \begin{cases} v_h|_K, & \forall K \in \mathcal{T}_{h,i}^\circ, \\ (E_{K_i^\circ} v_h)|_{K_i^\circ} & \forall K \in \mathcal{T}_h^\Gamma, \end{cases} \tag{5}$$

where K_i° is defined in Assumption 3. Note that for any cut element $K \in \mathcal{T}_h^\Gamma$, the operator $E_{h,i}$ extends polynomials of degree m from the assigned interior element K_i° to K.

Step 3. We define the approximation space $V_{h,i}^m$ as the image space of the operator $E_{h,i}$,

$$V_{h,i}^m := \{E_{h,i} v_h \mid \forall v_h \in V_{h,i}^{m,\circ}\}.$$

From (5), it can be seen that $V_{h,i}^m$ is a piecewise polynomial space and shares the same degrees of freedom and corresponding basis functions as the space $V_{h,i}^{m,\circ}$.

We present some properties of the space $V_{h,i}^m$, which are instrumental in the forthcoming analysis.

Lemma 1 *There exists a constant C such that for any $K \in \mathcal{T}_h^\Gamma$ and $i = 0, 1$, there holds*

$$\|D^q v_h\|_{L^2((\partial K)^i)} \le C h_K^{-1/2} \|D^q v_h\|_{L^2(K_i^\circ)}, \quad \forall v_h \in V_{h,i}^m, \quad q = 0, 1, \tag{6}$$

$$\|D^q v_h\|_{L^2(K^i)} \le \|D^q v_h\|_{L^2(K_i^\circ)}, \quad v_h \in V_{h,i}^m, \quad q = 0, 1. \tag{7}$$

Here we recall that $(\partial K)^i$ and K^i are respectively defined in (1) and (2), and that K_i° is the assigned neighbouring interior element of K with respect to Ω_i.

Proof From the mesh regularity, there exists a constant C_0 such that $C_\Delta \le (C_\Delta h_{K_i^\circ})/\rho_{K_i^\circ} \le C_0$. Considering the norm equivalence between $\|\cdot\|_{L^2(B(\boldsymbol{x}_{K_i^\circ}, C_0))}$ and $\|\cdot\|_{L^2(B(\boldsymbol{x}_{K_i^\circ}, 1))}$ for the space $\mathbb{P}_m(\cdot)$ and the affine mapping from $B(\boldsymbol{x}_{K_i^\circ}, 1)$ to the $B(\boldsymbol{x}_{K_i^\circ}, \rho_{K_i^\circ})$, there holds

$$\|D^q w_h\|_{L^2(B(\boldsymbol{x}_{K^\circ}, C_\Delta h_{K^\circ}))} \le C \|D^q w_h\|_{L^2(B(\boldsymbol{x}_{K^\circ}, \rho_{K^\circ}))}, \quad \forall w_h \in \mathbb{P}_m(B(\boldsymbol{x}_{K^\circ}, C_\Delta h_{K^\circ})). \tag{8}$$

By this estimate and the inverse estimate, we deduce that

$$\begin{aligned} \|D^q v_h\|_{L^2((\partial K)^i)} &\le |(\partial K)^i|^{1/2} \|D^q v_h\|_{L^\infty(B(\boldsymbol{x}_{K_i^\circ}, C_\Delta h_{K_i^\circ}))} \\ &\le |(\partial K)^i|^{1/2} h_{K_i^\circ}^{-d/2} \|D^q v_h\|_{L^2(B(\boldsymbol{x}_{K_i^\circ}, C_\Delta h_{K_i^\circ}))} \\ &\le C |(\partial K)^i|^{1/2} h_{K_i^\circ}^{-d/2} \|D^q v_h\|_{L^2(B(\boldsymbol{x}_{K_i^\circ}, \rho_{K_i^\circ}))} \\ &\le C |(\partial K)^i|^{1/2} h_{K_i^\circ}^{-d/2} \|D^q v_h\|_{L^2(K_i^\circ)} \le C h_K^{-1/2} \|D^q v_h\|_{L^2(K_i^\circ)}, \end{aligned}$$

where the last inequality follows the mesh regularity $C_1 h_K \le h_{K_i^\circ} \le C_2 h_K$ and the estimate $|(\partial K)^i| \le C h_K^{d-1}$ [47] due to the fact that Γ is C^2-smooth or polygonal. Similarly, we can prove the estimate (7). This completes the proof. □

Lemma 2 *There exists a constant C such that*

$$\sum_{e\in\mathcal{E}_{h,i}^{I}} h_e^{-1}\|[\![v_h]\!]\|_{L^2(e^i)}^2 \le C\Big(\sum_{K\in\mathcal{T}_{h,i}^{\circ}}\|\nabla v_h\|_{L^2(K)}^2 + \sum_{e\in\mathcal{E}_{h,i}^{\circ,I}} h_e^{-1}\|[\![v_h]\!]\|_{L^2(e)}^2\Big),\quad \forall v_h\in V_{h,i}^m. \tag{9}$$

Proof The proof follows the idea in [23, Appendix B]. We first show that

$$\sum_{e\in\mathcal{E}_{h}^{\Gamma}} h_e^{-1}\|[\![v_h]\!]\|_{L^2(e^i)}^2 \le C\Big(\sum_{K\in\mathcal{T}_{h,i}^{\circ}}\|\nabla v_h\|_{L^2(K)}^2 + \sum_{e\in\mathcal{E}_{h,i}^{\circ,I}} h_e^{-1}\|[\![v_h]\!]\|_{L^2(e)}^2\Big). \tag{10}$$

Here we verify it for the case $i=0$. From Assumption 4, for any face $e\in\mathcal{E}_h^{\Gamma}$ shared by two adjacent elements $\widehat{K}$ and $\widetilde{K}$, there exists a sequence of elements $K_0,\dots,K_M$ such that $K_0=(\widehat{K})_0^{\circ}$, $K_1=(\widetilde{K})_0^{\circ}$ and $K_j\in\mathcal{T}_{h,0}^{\circ}(1\le j\le M)$, and we let $e_j=\partial K_j\cap\partial K_{j+1}$. From the quasi-uniformity of $\mathcal{T}_h$, there exists a constant C_M such that the ball $B(\boldsymbol{x}_{K_0},C_Mh_{K_0})$ contains all K_j. We define v_h^j as the extension of $v_h|_{K_j}$ from the element K_j to the ball $B(\boldsymbol{x}_{K_0},C_Mh_{K_0})$. As (8), there exists a constant C such that

$$\|\nabla^q v\|_{L^2(K_j)}\le C\|\nabla^q v\|_{L^2(K_l)},\ \forall v\in\mathbb{P}_m(B(\boldsymbol{x}_{K_0},C_Mh_{K_0})),\ 1\le j,l\le M,\ q=0,1. \tag{11}$$

From the trace estimate and Lemma 1, we have that

$$h_e^{-1/2}\|[\![v_h]\!]\|_{L^2(e^0)}\le Ch_e^{-1}\|v_h^0-v_h^M\|_{L^2(\widehat{K})}\le Ch_{K_0}^{-1}\|v_h^0-v_h^M\|_{L^2(K_0)}.$$

By the norm equivalence over finite dimensional spaces [23], there holds

$$\|v_h^j-v_h^{j+1}\|_{L^2(K_j)}\le C(h_{e_j}^{1/2}\|[\![v_h]\!]\|_{L^2(e_j)}+h_{K_j}\|\nabla v_h^j-\nabla v_h^{j+1}\|_{L^2(K_j)}),\quad 1\le j\le M-1.$$

Then, from the estimate (11), we conclude that

$$\begin{aligned}
h_e^{-1}\|[\![v_h]\!]\|_{L^2(e^0)}^2 &\le Ch_{K_0}^{-2}\|v_h^0-v_h^M\|_{L^2(K_0)}^2\le C\sum_{j=0}^{M-1}h_{K_j}^{-2}\|v_h^j-v_h^{j+1}\|_{L^2(K_j)}^2\\
&\le C\sum_{j=0}^{M-1}(h_{e_j}^{-1}\|[\![v_h]\!]\|_{L^2(e_j)}^2+\|\nabla v_h^j-\nabla v_h^{j+1}\|_{L^2(K_j)}^2)\\
&\le C\sum_{j=0}^{M-1}(h_{e_j}^{-1}\|[\![v_h]\!]\|_{L^2(e_j)}^2+\|\nabla v_h\|_{L^2(K_j)}^2+\|\nabla v_h\|_{L^2(K_{j+1})}^2).
\end{aligned}$$

Summation over all cut faces gives us the estimate (10) with $i=0$. From the method of selecting K_0° and the definition of $E_{h,0}$, there holds $[\![v_h]\!]|_e=0$ on any $e\in\mathcal{E}_{h,0}^{\circ,B}$, which implies the estimate (9). The proof can be extended to the case $i=1$ without any difficulty. This completes the proof. □

Let $I_{h,i}$ be the corresponding Lagrange interpolation operator of the space $V_{h,i}^{m,\circ}$ and recall that Ω^* is an open bounded domain including the union of all balls $B(\boldsymbol{x}_K,C_\Delta h_K)$ $(\forall K\in\mathcal{T}_h)$. Then the following lemma shows the approximation property of the space $V_{h,i}^m$.

Lemma 3 *For any element $K\in\mathcal{T}_{h,i}^{\circ}$, there exists a constant C such that*

$$\|u-I_{h,i}u\|_{H^q(K)}\le Ch_K^{m+1-q}\|u\|_{H^{m+1}(K)},\quad q=0,1,\quad \forall u\in H^{m+1}(\Omega^*), \tag{12}$$

and for any element $K \in \mathcal{T}_h^{\Gamma}$, there exists a constant C such that

$$\|u - E_{h,i}(I_{h,i}u)\|_{H^q(K)} \le C h_K^{m+1-q} \|u\|_{H^{m+1}(B(\boldsymbol{x}_{K^\circ}, C_\Delta h_{K^\circ}))}, \quad q = 0, 1, \quad \forall u \in H^{m+1}(\Omega^*). \tag{13}$$

Proof It is sufficient to verify the estimate (13), since the estimate (12) is standard. For the ball $B(\boldsymbol{x}_{K_i^\circ}, C_\Delta h_{K_i^\circ})$, there exists a polynomial $v_h \in \mathbb{P}_m(B(\boldsymbol{x}_{K_i^\circ}, C_\Delta h_{K_i^\circ}))$ such that [8][8, Chapter 4]

$$\|u - v_h\|_{H^q(B(\boldsymbol{x}_{K_i^\circ}, C_\Delta h_{K_i^\circ}))} \le C h_{K_i^\circ}^{m+1-q} \|u\|_{H^{m+1}(B(\boldsymbol{x}_{K_i^\circ}, C_\Delta h_{K_i^\circ}))}.$$

Thus, we have that

$$\|u - E_{h,i}(I_{h,i}u)\|_{H^q(K)} \le \|u - v_h\|_{H^q(K)} + \|v_h - E_{h,i}(I_{h,i}u)\|_{H^q(K)}.$$

Combining $h_{K_i^\circ} \le C h_K$ and (8), the above result brings us that

$$\begin{aligned}
\|v_h - E_{h,i}(I_{h,i}u)\|_{H^q(K)} &= \|E_{h,i}(v_h - I_{h,i}u)\|_{H^q(K)} \le \|E_{h,i}(v_h - I_{h,i}u)\|_{H^q(B(\boldsymbol{x}_{K_i^\circ}, C h_{K_i^\circ}))} \\
&\le C\|v_h - I_{h,i}u\|_{H^q(B(\boldsymbol{x}_{K_i^\circ}, \rho_{K_i^\circ}))} \le C\|v_h - I_{h,i}u\|_{H^q(K_i^\circ)} \\
&\le C\left(\|u - v_h\|_{H^q(K_i^\circ)} + \|u - I_{h,i}u\|_{H^q(K_i^\circ)}\right) \\
&\le C h_K^{m+1-q} \|u\|_{H^{m+1}(B(\boldsymbol{x}_{K_i^\circ}, C h_{K_i^\circ}))},
\end{aligned}$$

which completes the proof. □

We have shown the definition and corresponding properties of the approximation space. The computer implementation is the extended space $V_{h,i}^m (i = 0, 1)$ is the same as common finite element spaces. We only need to implement the spaces $V_{h,i}^{m,\circ}$ on $\mathcal{T}_{h,i}^{\circ}$, and for cut elements, we directly use the basis functions of specified interior elements to assemble the stiffmatrix. We note that, for the space $V_{h,i}^m$, there is no need to calculate the nodal values on outer degrees of freedom to obtain the approximation space, which is different from the aggregated methods [5], and that the polynomials defined on the cut elements are just the same polynomials on the assigned interior elements in our method. The implementation of the space is very simple and does not need any strategy for adjusting the mesh to eliminate the effects of the small cuts. As a result, the curve Γ is allowed to intersect the partition in an arbitrary fashion. In next two sections, we will apply the spaces $V_{h,0}^m$ and $V_{h,1}^m$ to solve the elliptic problem on a curved domain and the elliptic interface problem.

We close this section by giving two fundamental results in unfitted methods. The first is the trace inequality on the curve Γ [27, 29, 47]:

Lemma 4 *There exists a constant h_0 independent of h such that if $0 < h \le h_0$, there exists a constant C such that*

$$\|w\|_{L^2(\Gamma_K)}^2 \le C\left(h_K^{-1}\|w\|_{L^2(K)}^2 + h_K\|w\|_{H^1(K)}^2\right), \quad \forall w \in H^1(K), \quad \forall K \in \mathcal{T}_h^{\Gamma}. \tag{14}$$

The second is the Sobolev extension theory [1]. For $i = 0, 1$, we assume there exists an extension operator $E_i : H^s(\Omega_i) \to H^s(\Omega^*)(s \ge 1)$ such that for any $w \in H^s(\Omega_i)$, there holds

$$(E_i w)|_{\Omega_i} = w, \quad \|E_i w\|_{H^q(\Omega^*)} \le C\|w\|_{H^q(\Omega_i)}, \quad 1 \le q \le s. \tag{15}$$

Hereafter, the condition $h \le h_0$ is assumed to be always fulfilled.

3 Approximation to Elliptic Problem on Curved Domain

In this section, we are concerned with the model boundary problem defined on the curved domain Ω_0: seek u such that

$$\begin{aligned} -\Delta u &= f, \quad \text{in } \Omega_0, \\ u &= g, \quad \text{on } \Gamma. \end{aligned} \tag{16}$$

We assume $f \in L^2(\Omega_0)$ and $g \in H^{3/2}(\Gamma)$. Then the problem (16) admits a unique solution $u \in H^2(\Omega_0)$ from the standard regularity result [19]. For this problem, the mesh $\mathcal{T}_h$ can be regarded as a background mesh and $\mathcal{T}_{h,0}$ is the computational mesh which is the minimal subset of $\mathcal{T}_h$ covering Ω_0. The trace operators in (3) for this problem are specified as

$$\{v\}|_{\Gamma_K} := v|_{\Gamma_K}, \quad [\![v]\!]|_{\Gamma_K} := v|_{\Gamma_K}\mathbf{n}, \quad \{\boldsymbol{q}\}|_{\Gamma_K} := \boldsymbol{q}|_{\Gamma_K}, \quad [\![\boldsymbol{q}]\!]|_{\Gamma_K} := \boldsymbol{q}|_{\Gamma_K} \cdot \mathbf{n},$$

for any $K \in \mathcal{T}_h^{\Gamma}$, where $\mathbf{n}$ denotes the unit outward normal vector on Γ.

We solve the problem (16) by the space $V_{h,0}^m$, and the numerical solution is sought by the following discrete variational form: find $u_h \in V_{h,0}^m$ such that

$$a_h(u_h, v_h) = l_h(v_h), \quad \forall v_h \in V_{h,0}^m, \tag{17}$$

where the bilinear form $a_h(\cdot,\cdot)$ takes the form

$$\begin{aligned} a_h(u_h, v_h) :=& \sum_{K\in\mathcal{T}_{h,0}} \int_{K^0} \nabla u_h \cdot \nabla v_h \mathrm{d}\boldsymbol{x} \\ &- \left(\sum_{e\in\mathcal{E}_h^{\Gamma}} \int_{e^0} + \sum_{K\in\mathcal{T}_h^{\Gamma}} \int_{\Gamma_K} \right) (\{\nabla u_h\} \cdot [\![v_h]\!] - \{\nabla v_h\} \cdot [\![u_h]\!]) \mathrm{d}\boldsymbol{s} \\ &+ \sum_{K\in\mathcal{T}_h^{\Gamma}} \int_{\Gamma_K} \mu h_K^{-1} [\![u_h]\!] \cdot [\![v_h]\!] \mathrm{d}\boldsymbol{s} + J_h(u_h, v_h), \\ J_h(u_h, v_h) :=& - \sum_{e\in\mathcal{E}_{h,0}^{\circ}} \int_e (\{\nabla u_h\} \cdot [\![v_h]\!] - \{\nabla v_h\} \cdot [\![u_h]\!]) \mathrm{d}\boldsymbol{s} \\ &+ \sum_{e\in\mathcal{E}_{h,0}^{\circ,I}} \int_e \mu h_e^{-1} [\![u_h]\!] \cdot [\![v_h]\!] \mathrm{d}\boldsymbol{s}, \end{aligned} \tag{18}$$

with μ the positive penalty parameter. The linear form $l_h(\cdot)$ reads

$$l_h(v_h) := \sum_{K\in\mathcal{T}_{h,0}} \int_{K^0} f v_h dx + \sum_{K\in\mathcal{T}_h^{\Gamma}} \int_{\Gamma_K} \{\nabla v_h\} \cdot \mathbf{n} g \mathrm{d}\boldsymbol{s} + \sum_{K\in\mathcal{T}_h^{\Gamma}} \int_{\Gamma_K} \mu h_K^{-1} [\![v_h]\!] \cdot \mathbf{n} g \mathrm{d}\boldsymbol{s}. \tag{19}$$

The bilinear form (18) is suitable for both cases that $V_{h,0}^{m,\circ}$ is the discontinuous piecewise polynomial space or the C^0 finite element space. If $V_{h,0}^{m,\circ}$ is the continuous space, $a_h(\cdot,\cdot)$ can be further simplified by $J_h(u_h, v_h) = 0$. We note that even if $V_{h,0}^{m,\circ}$ is the continuous space, $V_{h,0}^m$ is not continuous over the domain Ω_0, but we still only require the penalty terms defined on the boundary Γ under this case.

Next, we focus on the well-posedness of the discrete problem (17). For this goal, we introduce an energy norm $\|\cdot\|_{\mathrm{DG}}$ by

$$\|v_h\|_{\mathrm{DG}}^2 := \sum_{K\in\mathcal{T}_{h,0}} \|\nabla v_h\|_{L^2(K^0)}^2 + \sum_{e\in\mathcal{E}_{h,0}^I} h_e \|\{\nabla v_h\}\|_{L^2(e^0)}^2 + \sum_{e\in\mathcal{E}_{h,0}^I} h_e^{-1} \|[\![v_h]\!]\|_{L^2(e^0)}^2 + \sum_{K\in\mathcal{T}_h^\Gamma} h_K \|\{\nabla v_h\}\|_{L^2(\Gamma_K)}^2 + \sum_{K\in\mathcal{T}_h^\Gamma} h_K^{-1} \|[\![v_h]\!]\|_{L^2(\Gamma_K)}^2,$$

for any $v_h \in V_{h,0} := V_{h,0}^m + H^2(\Omega_0)$.

We show that the bilinear form $a_h(\cdot,\cdot)$ is bounded and coercive under the energy norm $\|\cdot\|_{\mathrm{DG}}$.

Lemma 5 *Let $a_h(\cdot,\cdot)$ be defined as (18) with any $\mu > 0$, there exist constants C such that*

$$|a_h(u_h, v_h)| \le C\|u_h\|_{\mathrm{DG}}\|v_h\|_{\mathrm{DG}}, \quad \forall u_h, v_h \in V_{h,0}, \tag{20}$$

$$a_h(v_h, v_h) \ge C\|v_h\|_{\mathrm{DG}}^2, \quad \forall v_h \in V_{h,0}^m. \tag{21}$$

Proof The boundedness (20) directly follows the Cauchy-Schwarz inequality. The rest is to prove the coercivity (21). We introduce a weaker norm $\|\cdot\|_*$, which is defined as

$$\|w_h\|_*^2 := \sum_{K\in\mathcal{T}_{h,0}} \|\nabla w_h\|_{L^2(K^0)}^2 + \sum_{e\in\mathcal{E}_{h,0}^{\circ,I}} h_e^{-1} \|[\![w_h]\!]\|_{L^2(e)}^2 + \sum_{K\in\mathcal{T}_h^\Gamma} h_K^{-1} \|[\![w_h]\!]\|_{L^2(\Gamma_K)}^2, \quad \forall w_h \in V_{h,0}^m.$$

From the definition of $a_h(\cdot,\cdot)$, the coercivity (21) is equal to the equivalence between the norms $\|\cdot\|_{\mathrm{DG}}$ and $\|\cdot\|_*$ restricted on the approximation space $V_{h,0}^m$. Obviously, it suffices to prove $\|w_h\|_{\mathrm{DG}} \le C\|w_h\|_*$. From Lemma 2, we have that $\sum_{e\in\mathcal{E}_{h,0}^I} h_e^{-1}\|[\![w_h]\!]\|_{L^2(e^0)}^2 \le C\|w_h\|_*^2$. By the standard trace estimate and the estimate (7), we derive that

$$\sum_{e\in\mathcal{E}_{h,0}^I} h_e \|\{\nabla w_h\}\|_{L^2(e^0)}^2 \le C \sum_{K\in\mathcal{T}_{h,0}} \|\nabla w_h\|_{L^2(K)}^2 \le C \sum_{K\in\mathcal{T}_{h,0}^\circ} \|\nabla w_h\|_{L^2(K)}^2 \le C\|w_h\|_*^2,$$

and by the trace estimate (6), we obtain that

$$\sum_{K\in\mathcal{T}_h^\Gamma} h_K \|\{\nabla w_h\}\|_{L^2(\Gamma_K)}^2 \le \sum_{K\in\mathcal{T}_h^\Gamma} C\|\nabla w_h\|_{L^2(K_0^\circ)}^2 \le C\|w_h\|_*^2.$$

Collecting the above estimates immediately indicates $\|w_h\|_{\mathrm{DG}} \le C\|w_h\|_*$. Thus, there holds $a_h(v_h, v_h) \ge C\|v_h\|_*^2 \ge C\|v_h\|_{\mathrm{DG}}^2$, which completes the proof. □

The Galerkin orthogonality holds for the bilinear form $a_h(\cdot,\cdot)$ and linear form $l_h(\cdot)$.

Lemma 6 *Let $u \in H^2(\Omega)$ be the exact solution to problem (16), and let $u_h \in V_h^m$ be the numerical solution to problem (17), there holds*

$$a_h(u - u_h, v_h) = 0, \quad \forall v_h \in V_{h,0}^m. \tag{22}$$

Proof From the regularity of u, we have $[\![u]\!]|_e = 0$ for any face $e \in \mathcal{E}^I_{h,0}$. We bring u into the bilinear form $a_h(\cdot,\cdot)$ and get

$$a(u, v_h) - l(v_h) = \sum_{K\in\mathcal{T}_{h,0}} \int_{K^0} (\nabla u \cdot \nabla v_h - f v_h) \mathrm{d}\boldsymbol{x} - \sum_{e\in\mathcal{E}^I_{h,0}} \int_{e^0} \nabla u \cdot [\![v_h]\!] \mathrm{d}\boldsymbol{s} - \sum_{K\in\mathcal{T}^\Gamma_h} \int_{\Gamma_K} \nabla u \cdot [\![v_h]\!] \mathrm{d}\boldsymbol{s}.$$

Applying integration by parts leads to

$$\sum_{K\in\mathcal{T}^\circ_{h,0}} \int_K (\nabla u \cdot \nabla v_h - f v_h) \mathrm{d}\boldsymbol{x} = \sum_{e\in\mathcal{E}^\circ_{h,0}} \int_e \nabla u \cdot [\![v_h]\!] \mathrm{d}\boldsymbol{s},$$

$$\sum_{K\in\mathcal{T}^\Gamma_h} \int_{K^0} (\nabla u \cdot \nabla v_h - f v_h) \mathrm{d}\boldsymbol{x} = \sum_{e\in\mathcal{E}^\Gamma_h} \int_{e^0} \nabla u \cdot [\![v_h]\!] \mathrm{d}\boldsymbol{s} + \sum_{K\in\mathcal{T}^\Gamma_h} \int_{\Gamma_K} \nabla u \cdot [\![v_h]\!] \mathrm{d}\boldsymbol{s},$$

which indicate $a(u, v_h) - l(v_h) = 0$ and the Galerkin orthogonality (22). This completes the proof. □

Combining the approximation properties (12) and (13), the trace estimate (14), and the Sobolev extension operator E_0, we claim the following approximation estimate under the error measurement $\|\cdot\|_{\mathrm{DG}}$:

Theorem 1 *There exists a constant C such that*

$$\inf_{v_h\in V^m_{h,0}} \|u - v_h\|_{\mathrm{DG}} \le C h^m \|u\|_{H^{m+1}(\Omega_0)}, \quad \forall u \in H^{m+1}(\Omega_0). \tag{23}$$

Proof Let $I_{h,0}(E_0u)$ be the Lagrange interpolant of E_0u into the space $V^{m,\circ}_{h,0}$ and consider $v_h = E_{h,0}(I_{h,0}u)$. From Lemma 3, we have that

$$\sum_{K\in\mathcal{T}_{h,0}} \|E_0u - v_h\|_{H^q(K)} \le C h^{m+1-q} \|E_0u\|_{H^{m+1}(\Omega^*)} \le C h^{m+1-q} \|u\|_{H^{m+1}(\Omega_0)},$$

with $0 \le q \le 2$. From the standard trace estimate, we conclude that

$$\begin{aligned}\sum_{e\in\mathcal{E}^I_{h,0}} h_e \|\{\nabla u - \nabla v_h\}\|^2_{L^2(e^0)} &\le C \sum_{K\in\mathcal{T}_{h,0}} (\|E_0u - v_h\|^2_{H^1(K)} + h_K^2 \|E_0u - v_h\|^2_{H^2(K)}) \\ &\le C h^{2m} \|E_0u\|^2_{H^{m+1}(\Omega^*)} \le C h^{2m} \|u\|^2_{H^{m+1}(\Omega_0)}.\end{aligned}$$

We apply the trace estimate (14) to see that

$$\begin{aligned}\sum_{K\in\mathcal{T}^\Gamma_h} h_K \|\{\nabla u - \nabla v_h\}\|^2_{L^2(\Gamma_K)} &\le C \sum_{K\in\mathcal{T}^\Gamma_h} (\|E_0u - v_h\|^2_{H^1(K)} + h_K^2 \|E_0u - v_h\|^2_{H^2(K)}) \\ &\le C h^{2m} \|u\|^2_{H^{m+1}(\Omega_0)}.\end{aligned}$$

It is similar to bound other terms of $\|u - v_h\|_{\mathrm{DG}}$, which gives the estimate (23) and completes the proof. □

Now, we are ready to give an *a priori* error estimate for our method.

Theorem 2 *Let $u \in H^{m+1}(\Omega_0)$ be the exact solution to (16) and $u_h \in V_{h,0}^m$ be the numerical solution to (17), and let $a_h(\cdot,\cdot)$ be defined as (18) with any $\mu > 0$, then there exists a constant C such that*

$$\|u - u_h\|_{\mathrm{DG}} \le Ch^m \|u\|_{H^{m+1}(\Omega_0)}. \tag{24}$$

Proof The proof follows from the standard Lax-Milgram framework. For any $v_h \in V_{h,0}^m$, combining the boundedness (20), the coercivity (21), and the Galerkin orthogonality (22) gives

$$\begin{aligned}\|u_h - v_h\|_{\mathrm{DG}}^2 &\le Ca_h(u_h - v_h, u_h - v_h) = Ca_h(u - v_h, u_h - v_h)\\ &\le C\|u_h - v_h\|_{\mathrm{DG}}\|u - v_h\|_{\mathrm{DG}}.\end{aligned}$$

Applying the triangle inequality and the approximation estimate (23) yields the error estimate (24). This completes the proof. □

Remark 3 From the estimate (25), we can further give the suboptimal convergence rate under the L^2 norm. The scheme (17) can be termed as a non-symmetric interior penalty method. For the non-symmetric bilinear form, the odd/even situation usually can be numerically detected for the L^2 error, i.e. the numerical error under the L^2 norm decreases to zero at the optimal/suboptimal rate for the odd/even approximation accuracy, and the theoretical verification is still an open problem [3, 17, 24, 34]. But for our method, the numerical results reveal the optimal convergence for the L^2 error for all m.

In the rest of this section, we give an upper bound of the condition number of the final sparse linear system, which is still independent of how the boundary Γ cuts the mesh. The main ingredient is to prove a Poincaré-type inequality.

Lemma 7 *There exist constants C such that*

$$\begin{aligned}\|v_h\|_{L^2(\Omega)} &\le C\|v_h\|_{\mathrm{DG}}, &&\forall v_h \in V_{h,0},\\ \|v_h\|_{\mathrm{DG}} &\le Ch^{-1}\|v_h\|_{L^2(\Omega)}, &&\forall v_h \in V_{h,0}^m.\end{aligned} \tag{25}$$

Proof For any $v_h \in V_{h,0}$, we apply the duality argument to show $\|v_h\|_{L^2(\Omega_0)} \le C\|v_h\|_{\mathrm{DG}}$. Let $\phi \in H^2(\Omega_0)$ be the solution of the problem

$$-\Delta\phi = v_h, \text{ in } \Omega_0, \quad \phi = 0, \text{ on } \partial\Omega_0,$$

with $\|\phi\|_{H^2(\Omega_0)} \le C\|v_h\|_{L^2(\Omega_0)}$. Applying integration by parts, we find that

$$\begin{aligned}\|v_h\|_{L^2(\Omega_0)}^2 &= (-\Delta\phi, v_h)_{L^2(\Omega_0)}\\ &= \sum_{K\in\mathcal{T}_{h,0}} (\nabla\phi, \nabla v_h)_{L^2(K^0)} - \sum_{e\in\mathcal{E}_{h,0}} (\nabla\phi, [\![v_h]\!])_{L^2(e^0)} - \sum_{K\in\mathcal{T}_h^\Gamma} (\nabla\phi, [\![v_h]\!])_{L^2(\Gamma_K)}\\ &\le C\|v_h\|_{\mathrm{DG}}\Big(|\nabla\phi|_{L^2(\Omega)}^2 + \sum_{e\in\mathcal{E}_{h,0}} h_e|\nabla\phi|_{L^2(e^0)}^2 + \sum_{K\in\mathcal{T}_h^\Gamma} h_K|\nabla\phi|_{L^2(\Gamma_K)}^2\Big)^{1/2}.\end{aligned}$$

From Lemma 4 and the trace estimate, we deduce

$$\sum_{K\in\mathcal{T}_h^\Gamma} h_K|\nabla\phi|_{L^2(\Gamma_K)}^2 \le C\sum_{K\in\mathcal{T}_h^\Gamma} \|E_0\phi\|_{H^2(K)}^2 \le C\|\phi\|_{H^2(\Omega_0)}^2,$$

and

$$\sum_{e\in\mathcal{E}_{h,0}} h_e|\nabla\phi|^2_{L^2(e^0)} \le \sum_{e\in\mathcal{E}_{h,0}} h_e|\nabla(E_0\phi)|^2_{L^2(e)} \le C\sum_{K\in\mathcal{T}_{h,0}} \|E_0\phi\|^2_{H^2(K)} \le C\|\phi\|^2_{H^2(\Omega_0)}.$$

These two inequalities, together with the regularity of ϕ, imply $\|v_h\|_{L^2(\Omega_0)} \le C\|v_h\|_{\mathrm{DG}}$. For any $v_h \in V^m_{h,0}$, the inequality $\|v_h\|_{\mathrm{DG}} \le Ch^{-1}\|v_h\|_{L^2(\Omega_0)}$ directly follows the inverse inequality and Lemma 1, which completes the proof. □

Let $\{\phi_i\}(1 \le i \le n)$ be the Lagrange basis of the space $V^{m,\circ}_{h,0}$. Clearly, $V^m_{h,0}$ shares the same degrees of freedom and corresponding basis functions as those of $V^{m,\circ}_{h,0}$. Let $A = (a_h(\phi_i, \phi_j))_{n\times n}$ be the resulting stiff matrix. We further let S and N be the matrices with respect to the following bilinear forms $a^S_h(\cdot,\cdot)$ and $a^N_h(\cdot,\cdot)$, which read

$$\begin{aligned}
a^S_h(u_h, v_h) :=& \sum_{K\in\mathcal{T}_{h,0}} \int_{K^0} \nabla u_h\cdot\nabla v_h \mathrm{d}\boldsymbol{x} + \sum_{e\in\mathcal{E}^{\circ,I}_{h,0}} \int_e \mu h_e^{-1}[\![u_h]\!]\cdot[\![v_h]\!]\mathrm{d}s \\
&+ \sum_{K\in\mathcal{T}^\Gamma_h} \int_{\Gamma_K} \mu h_K^{-1}[\![u_h]\!]\cdot[\![v_h]\!]\mathrm{d}s, \quad \forall u_h, v_h \in V^m_h, \\
a^N_h(u_h, v_h) :=& \sum_{e\in\mathcal{E}^I_{h,0}} \int_{e^0} (\{\nabla u_h\}\cdot[\![v_h]\!] - \{\nabla v_h\}\cdot[\![u_h]\!])\mathrm{d}s, \\
&+ \sum_{K\in\mathcal{T}^\Gamma_h} \int_{\Gamma_K} (\{\nabla u_h\}\cdot[\![v_h]\!] - \{\nabla v_h\}\cdot[\![u_h]\!])\mathrm{d}s, \quad \forall u_h, v_h \in V^m_h.
\end{aligned}$$

Clearly, we have that $A = S - N$, and $a^S_h(\cdot,\cdot)$ and $a^N_h(\cdot,\cdot)$ indeed represent the symmetric and antisymmetric part of the bilinear form $a_h(\cdot,\cdot)$.

Theorem 3 *There exists a constant C such that*

$$\kappa(A) \le Ch^{-2}. \tag{26}$$

Proof Since S is symmetric, all of eigenvalues of S are real and we can further show that

$$C \le h^{-d}\lambda_{\min}(S) \le h^{-d}\lambda_{\max}(S) \le Ch^{-2}. \tag{27}$$

For any vector $\mathbf{v} = (v_1, v_2, \ldots, v_n)^T \in \mathbb{R}^n$, we let $v_h = \sum_{i=1}^n v_i\phi_i$. To verify (27), we seek the lower and upper bounds of $(\mathbf{v}^T S\mathbf{v})/(\mathbf{v}^T\mathbf{v})(\mathbf{v} \ne \mathbf{0})$ by

$$\frac{\mathbf{v}^T S\mathbf{v}}{\mathbf{v}^T\mathbf{v}} = \frac{a^S_h(v_h, v_h)}{\|v_h\|^2_{L^2(\Omega_0)}} \frac{\|v_h\|^2_{L^2(\Omega_0)}}{\mathbf{v}^T\mathbf{v}}.$$

Clearly, $a^S_h(v_h, v_h) = a_h(v_h, v_h)$, together with Lemma 5 and Lemma 7, we have that $\|v_h\|^2_* \le Ca^S_h(v_h, v_h) \le C\|v_h\|^2_*$ and

$$C_1\|v_h\|^2_{L^2(\Omega_0)} \le a_h(v_h, v_h) \le C_2h^{-2}\|v_h\|^2_{L^2(\Omega_0)}.$$

Since $\mathbf{v}$ corresponds to the degrees of freedom of the standard finite element space $V^{m,\circ}_{h,0}$, we can know that

$$C_1\|v_h\|^2_{L^2(\mathcal{T}^\circ_{h,0})} \le h^d(\mathbf{v}^T\mathbf{v}) \le C_2\|v_h\|^2_{L^2(\mathcal{T}^\circ_{h,0})}.$$

From Lemma 1, there holds $\|v_h\|_{L^2(\Omega_0)} \le C\|v_h\|_{L^2(\mathcal{T}_{h,0}^\circ)} \le C\|v_h\|_{L^2(\Omega_0)}$. By the Raleigh quotient formula, we can obtain the bound (27).

We note that N is antisymmetric and all eigenvalues of N are purely imaginary. We then show the spectral radius of N satisfies that $h^{-d}\rho(N) \le Ch^{-2}$. Again from Lemma 5 and 7, we find that

$$a_h^N(v_h, w_h) \le C\|v_h\|_{\mathrm{DG}}\|w_h\|_{\mathrm{DG}} \le Ch^{-2}\|v_h\|_{L^2(\Omega_0)}\|w_h\|_{L^2(\Omega_0)}, \quad \forall v_h, w_h \in V_{h,0}^m.$$

Hence, for any $\mathbf{v}, \mathbf{w} \in \mathbb{R}^n$ with $\mathbf{v}^T\mathbf{v} = \mathbf{w}^T\mathbf{w} = 1$, we obtain that $h^{-d}(\mathbf{v}^T N\mathbf{w}) \le Ch^{-2}$, which gives $h^{-d}\rho(N) \le Ch^{-2}$. Together with the bounds of eigenvalues of S and the spectral radius of N, we can find $\kappa(A) \le Ch^{-2}$, which completes the proof. □

We have shown that the unfitted scheme (17) for the problem (16) is stable and can achieve an arbitrarily high order accuracy without any mesh adjustment or any special stabilization technique. In next section, we will extend this method to the elliptic interface problem.

4 Approximation to Elliptic Interface Problem

In this section, we are concerned with the following elliptic interface problem: seek u such that

$$\begin{aligned} -\nabla\cdot(\alpha\nabla u) &= f, && \text{in } \Omega_0 \cup \Omega_1,\\ u &= g, && \text{on } \partial\Omega,\\ [\![u]\!] &= a\mathbf{n}, && \text{on } \Gamma,\\ [\![\alpha\nabla u]\!] &= b, && \text{on } \Gamma. \end{aligned} \tag{28}$$

Here the domain Ω can be regarded as being divided by the C^2-smooth interface Γ into two disjoint subdomains Ω_0 and Ω_1. The data functions are assumed to satisfy that $f \in L^2(\Omega)$, $g \in H^{3/2}(\partial\Omega)$, $a \in H^{3/2}(\Gamma)$ and $b \in H^{1/2}(\Gamma)$, which make (28) possess a unique solution $u \in H^2(\Omega_0 \cup \Omega_1)$. We refer to [31, 32] for more regularity results to such an interface problem.

In this section, the trace operators (3) on the interface Γ are specified as

$$\{v\}|_{\Gamma_K} := \frac{1}{2}(v^0|_{\Gamma_K} + v^1|_{\Gamma_K}), \quad [\![v]\!]|_{\Gamma_K} := (v^0 - v^1)\mathbf{n},$$
$$\{\boldsymbol{q}\}|_{\Gamma_K} := \frac{1}{2}(\boldsymbol{q}^0|_{\Gamma_K} + \boldsymbol{q}^1|_{\Gamma_K}), \quad [\![\boldsymbol{q}]\!]|_{\Gamma_K} := (\boldsymbol{q}^0 - \boldsymbol{q}^1)\cdot\mathbf{n},$$

for any $K \in \mathcal{T}_h^\Gamma$, where $v^0 = v|_{K^0}$, $v^1 = v|_{K^1}$, $\boldsymbol{q}^0 = \boldsymbol{q}|_{K^0}$, $\boldsymbol{q}^1 = \boldsymbol{q}|_{K^1}$ and $\mathbf{n}$ denotes the unit normal vector on Γ_K pointing to Ω_1.

For the interface problem (28), the approximation space V_h^m is a combination of the spaces $V_{h,0}^m$ and $V_{h,1}^m$, which is defined as

$$V_h^m := V_{h,0}^m \cdot \chi_0 + V_{h,1}^m \cdot \chi_1,$$

where χ_i is the characteristic function corresponding to the subdomain Ω_i. Clearly, any function $v_h \in V_h^m$ admits the decomposition $v_h = v_{h,0}\cdot\chi_0 + v_{h,1}\cdot\chi_1$, where $v_h|_{\Omega_0} = v_{h,0}|_{\Omega_0}$ and $v_h|_{\Omega_1} = v_{h,1}|_{\Omega_1}$. In addition, the degrees of freedom of V_h^m are formed by all degrees of freedom of $V_{h,0}^{m,\circ}$ and $V_{h,1}^{m,\circ}$, which are entirely located in Ω_0 and Ω_1, respectively.

The discrete variational problem for (28) reads: seek $u_h \in V_h^m$ such that

$$a_h(u_h, v_h) = l_h(v_h), \quad \forall v_h \in V_h^m, \tag{29}$$

where

$$
\begin{aligned}
a_h(u_h, v_h) := & \sum_{K\in\mathcal{T}_h}\int_{K^0\cup K^1}\alpha\nabla u_h\cdot\nabla v_h\mathrm{d}\boldsymbol{x} \\
& -\left(\sum_{e\in\mathcal{E}_h^\Gamma}\int_{e^0\cup e^1}+\sum_{K\in\mathcal{T}_h^\Gamma}\int_{\Gamma_K}\right)(\{\alpha\nabla u_h\}\cdot[\![v_h]\!]-\{\alpha\nabla v_h\}\cdot[\![u_h]\!])\mathrm{d}\boldsymbol{s} \\
& +\sum_{K\in\mathcal{T}_h^\Gamma}\int_{\Gamma_K}\eta h_K^{-1}[\![u_h]\!]\cdot[\![v_h]\!]\mathrm{d}\boldsymbol{s}+J_h(u_h, v_h), \\
J_h(u_h, v_h) := & \sum_{e\in\mathcal{E}_{h,0}^\circ\cup\mathcal{E}_{h,1}^\circ}\int_{e^0\cup e^1}(\{\alpha\nabla u_h\}\cdot[\![v_h]\!]-\{\alpha\nabla v_h\}\cdot[\![u_h]\!])\mathrm{d}\boldsymbol{s} \\
& +\sum_{e\in\mathcal{E}_{h,0}^{\circ,I}\cup\mathcal{E}_{h,1}^{\circ,I}}\int_{e^0\cup e^1}\eta h_e^{-1}[\![u_h]\!]\cdot[\![v_h]\!]\mathrm{d}\boldsymbol{s},
\end{aligned}
\tag{30}
$$

with η the positive penalty parameter, and

$$
\begin{aligned}
l_h(v_h) := & \sum_{K\in\mathcal{T}_h}\int_{K^0\cup K^1}fv_h\mathrm{d}\boldsymbol{x}+\sum_{e\in\mathcal{E}_h^B}\int_e\{\alpha\nabla v_h\}\cdot\mathbf{n}g\mathrm{d}\boldsymbol{s}+\sum_{e\in\mathcal{E}_h^B}\int_e\eta h_e^{-1}gv_h\mathrm{d}\boldsymbol{s} \\
& +\sum_{K\in\mathcal{T}_h^\Gamma}\int_{\Gamma_K}b\{v_h\}\mathrm{d}\boldsymbol{s}+\sum_{K\in\mathcal{T}_h^\Gamma}\int_{\Gamma_K}\{\alpha\nabla v_h\}\cdot\mathbf{n}a\mathrm{d}\boldsymbol{s}+\sum_{K\in\mathcal{T}_h^\Gamma}\int_{\Gamma_K}\eta h_K^{-1}[\![v_h]\!]\cdot\mathbf{n}a\mathrm{d}\boldsymbol{s}.
\end{aligned}
$$

Similar as (18), $J_h(u_h, v_h)=0$ if $V_{h,0}^{m,\circ}$ and $V_{h,1}^{m,\circ}$ are C^0 finite element spaces.

Then we present the error estimation to the problem (29). We introduce the energy norm $|\!|\!|\cdot|\!|\!|_{\mathrm{DG}}$ on $V_h := V_h^m + H^2(\Omega_0\cup\Omega_1)$:

$$
\begin{aligned}
|\!|\!|v_h|\!|\!|_{\mathrm{DG}}^2 := & \sum_{K\in\mathcal{T}_h}\|\nabla v_h\|_{L^2(K^0\cup K^1)}^2+\sum_{e\in\mathcal{E}_h}h_e\|\{\nabla v_h\}\|_{L^2(e^0\cup e^1)}^2+\sum_{e\in\mathcal{E}_h}h_e^{-1}\|[\![v_h]\!]\|_{L^2(e^0\cup e^1)}^2 \\
& +\sum_{K\in\mathcal{T}_h^\Gamma}h_K\|\{\nabla v_h\}\|_{L^2(\Gamma_K)}^2+\sum_{K\in\mathcal{T}_h^\Gamma}h_K^{-1}\|[\![v_h]\!]\|_{L^2(\Gamma_K)}^2,
\end{aligned}
$$

for any $v_h\in V_h$.

We claim that the bilinear form $a_h(\cdot,\cdot)$ is bounded and coercive with respect to the energy norm $|\!|\!|\cdot|\!|\!|_{\mathrm{DG}}$.

Lemma 8 *Let $a_h(\cdot,\cdot)$ be defined as (30) with any $\eta>0$, then there exist constants C such that*

$$
|a_h(u, v)|\le C|\!|\!|u|\!|\!|_{\mathrm{DG}}|\!|\!|v|\!|\!|_{\mathrm{DG}},\quad \forall u, v\in V_h, \tag{31}
$$

$$
a_h(v_h, v_h)\ge C|\!|\!|v_h|\!|\!|_{\mathrm{DG}}^2,\quad \forall v_h\in V_h^m. \tag{32}
$$

Proof The proof is analogous to the proof of Lemma 5. Applying the Cauchy-Schwarz inequality and the definition of $|\!|\!|\cdot|\!|\!|_{\mathrm{DG}}$ immediately gives the estimate (31).

To obtain the coercivity (32), we also introduce a weaker norm $|||\cdot|||_*$,

$$|||w_h|||_*^2 := \sum_{K\in\mathcal{T}_h} \|\nabla w_h\|^2_{L^2(K^0\cup K^1)} + \sum_{e\in\mathcal{E}_h} h_e^{-1}\|[\![w_h]\!]\|^2_{L^2(e^0\cup e^1)} + \sum_{K\in\mathcal{T}_h^\Gamma} h_K^{-1}\|[\![w_h]\!]\|^2_{L^2(\Gamma_K)},$$

for any $w_h \in V_h^m$. The equivalence between $\|\cdot\|_{\mathrm{DG}}$ and $\|\cdot\|_*$ in Lemma 5 can be easily extended to $|||\cdot|||_{\mathrm{DG}}$ and $|||\cdot|||_*$. Hence, there holds $a_h(v_h, v_h) \geq C|||v_h|||_*^2 \geq C|||v_h|||_{\mathrm{DG}}^2$, which completes the proof. □

The proof of Lemma 6 also gives the Galerkin orthogonality for this problem.

Lemma 9 *Let $u \in H^2(\Omega_0\cup\Omega_1)$ be the exact solution to the problem (28), and let $u_h \in V_h^m$ be the numerical solution to the problem (29), then there holds*

$$a_h(u-u_h, v_h) = 0, \quad \forall v_h \in V_h^m.$$

Then we state the approximation property of the space V_h^m.

Theorem 4 *There exists a constant C such that*

$$\inf_{v_h\in V_h^m} |||u-v_h|||_{\mathrm{DG}} \leq Ch^m\|u\|_{H^{m+1}(\Omega_0\cup\Omega_1)}, \quad \forall u \in H^{m+1}(\Omega_0\cup\Omega_1). \tag{33}$$

Proof The estimate (33) is based on the extension operators $E_i\,(i=0,1)$ and Lemma 4, and the proof follows from the same line as in the proof of Theorem 1. □

Let us give an *a priori* error estimate for the proposed method.

Theorem 5 *Let $u \in H^{m+1}(\Omega_0\cup\Omega_1)$ be the exact solution to (28) and $u_h \in V_h^m$ be the numerical solution to (29), and let $a_h(\cdot,\cdot)$ be defined as (30) with any $\eta > 0$, then there exists a constant C such that*

$$|||u-u_h|||_{\mathrm{DG}} \leq Ch^m\|u\|_{H^{m+1}(\Omega_0\cup\Omega_1)}. \tag{34}$$

Proof The estimate (34) can be obtained by following the same line as in the proof of (24) under the Lax-Milgram framework based on Lemma 8, 9 and Theorem 4. □

Remark 4 For the interface problem (28), we can only prove the suboptimal convergence rate for the L^2 error. The numerical results demonstrate that for all m, $\|\cdot\|_{L^2(\Omega)}$ converges to zero at the optimal rates. For the proposed non-symmetric bilinear form (30), there is also no odd/even situation for the L^2 error; see Remark 3 for more details.

Ultimately, we present the estimate of the condition number for the discrete system (29). The main step is to give the bound for the energy norm $|||\cdot|||_{\mathrm{DG}}$.

Lemma 10 *There exist constants C such that*

$$\begin{aligned} \|v_h\|_{L^2(\Omega)} &\leq C|||v_h|||_{\mathrm{DG}}, && \forall v_h \in V_h, \\ |||v_h|||_{\mathrm{DG}} &\leq Ch^{-1}\|v_h\|_{L^2(\Omega)}, && \forall v_h \in V_h^m. \end{aligned} \tag{35}$$

Proof We also apply the dualduality argument to show that $\|v_h\|_{L^2(\Omega)} \le C|||v_h|||_{\mathrm{DG}}$ for any $v_h \in V_h$. Let $\phi \in H^2(\Omega_0 \cup \Omega_1)$ solve the interface problem

$$\begin{aligned} -\nabla \cdot \nabla \phi &= v_h, \quad \text{in } \Omega_0 \cup \Omega_1, \\ \phi &= 0, \quad \text{on } \partial\Omega, \\ [\![\phi]\!] &= 0, \quad \text{on } \Gamma, \\ [\![\nabla\phi]\!] &= 0, \quad \text{on } \Gamma, \end{aligned}$$

with the regularity $\|\phi\|_{H^2(\Omega)} \le C\|v_h\|_{L^2(\Omega)}$. From the integration by parts, we find that

$$\begin{aligned} \|v_h\|^2_{L^2(\Omega)} &= (-\nabla\cdot\nabla\phi, v_h)_{L^2(\Omega)} \\ &= \sum_{K\in\mathcal{T}_h} (\nabla\phi, \nabla v_h)_{L^2(K^0\cup K^1)} - \sum_{e\in\mathcal{E}_h} (\nabla\phi, [\![v_h]\!])_{L^2(e^0\cup e^1)} - \sum_{K\in\mathcal{T}_h^\Gamma} (\nabla\phi, [\![v_h]\!])_{L^2(\Gamma_K)} \\ &\le C|||v_h|||_{\mathrm{DG}} \left(\sum_{K\in\mathcal{T}_h} \|\nabla\phi\|^2_{L^2(K^0\cup K^1)} + \sum_{e\in\mathcal{E}_h} h_e\|\nabla\phi\|^2_{L^2(e)} + \sum_{K\in\mathcal{T}_h^\Gamma} h_K\|\nabla\phi\|^2_{L^2(\Gamma_K)} \right)^{1/2}. \end{aligned}$$

From the trace estimate, we have

$$\sum_{e\in\mathcal{E}_h} h_e\|\nabla\phi\|^2_{L^2(e)} \le C\|\phi\|^2_{H^2(\Omega)}, \quad \sum_{K\in\mathcal{T}_h^\Gamma} h_K\|\nabla\phi\|^2_{L^2(\Gamma_K)} \le C\|\phi\|^2_{H^2(\Omega)},$$

which give $\|v_h\|_{L^2(\Omega)} \le C|||v_h|||_{\mathrm{DG}}$. Moreover, it is easy to verify $|||v_h|||_{\mathrm{DG}} \le h^{-1}\|v_h\|_{L^2(\Omega)}$ for any $v_h \in V_h^m$ by the inverse estimate. This completes the proof. □

Theorem 6 *There exists a constant C such that*

$$\kappa(A) \le Ch^{-2}, \tag{36}$$

where A denotes the resulting stiff matrix of the discrete system (29).

Proof The estimate (36) is a consequence of Lemma 10; see the proof of Theorem 3. □

The unfitted method in Sect. 3 has been extended to the interface problem. The used approximation space V_h^m is easily implemented, since its basis functions come from two common finite element spaces. This method neither requires any constraint on how the interface intersects the mesh nor includes any special stabilization item.

5 Numerical Results

In this section, a series of numerical results are presented to illustrate the performance of the methods proposed in Sects. 3 and 4. In all tests, the data functions g, f in (16), as well as the functions g, f, a, b in (28), are taken suitably from the exact solution. The boundary or the interface for each case is described by a level set function ϕ. We note that the scheme involves the numerical integration on the intersections of the boundary/interface with elements. We refer to [15, 44] for some methods to seek the quadrature rules on curved domains. In our computation, the method in [15] is used (the codes are freely available online). For all tests, we adopt the BiCGSTAB solver together with the ILU preconditioner to solve the resulting linear algebraic system.

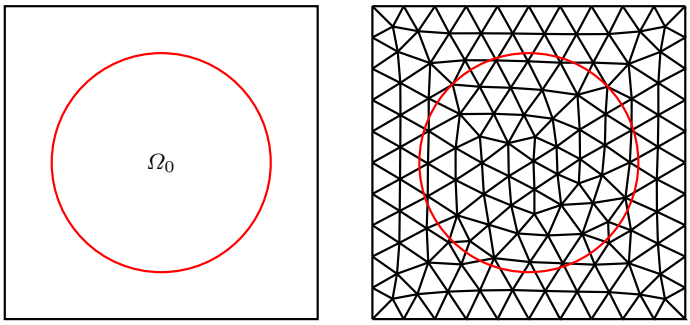

Fig. 3 The curved domain and the partition of Example 1

Table 1 Numerical errors of Example 1

m	h	1/5	1/10	order	1/20	order	1/40	order
1	$\|\boldsymbol{u}-\boldsymbol{u}_h\|_{L^2(\Omega_0)}$	4.442e−1	1.329e−1	1.73	3.328e−2	2.00	7.272e−3	2.19
	$\|\boldsymbol{u}-\boldsymbol{u}_h\|_{\mathrm{DG}}$	6.587e−0	3.520e−0	0.90	1.908e−0	1.03	8.189e−1	1.06
2	$\|\boldsymbol{u}-\boldsymbol{u}_h\|_{L^2(\Omega_0)}$	7.192e−2	1.443e−2	2.32	1.212e−3	3.57	1.422e−4	3.11
	$\|\boldsymbol{u}-\boldsymbol{u}_h\|_{\mathrm{DG}}$	2.172e−0	7.416e−1	1.55	1.451e−1	2.35	3.292e−2	2.13
3	$\|\boldsymbol{u}-\boldsymbol{u}_h\|_{L^2(\Omega_0)}$	1.661e−2	1.453e−3	3.51	8.262e−5	4.13	5.222e−6	4.01
	$\|\boldsymbol{u}-\boldsymbol{u}_h\|_{\mathrm{DG}}$	7.032e−1	8.976e−2	2.96	9.809e−3	3.19	1.088e−3	3.17

5.1 Convergence Studies for Elliptic Problems

We present several numerical examples to demonstrate the convergence rates of the unfitted method (17) for the problem (16). To obtain the approximation space $V_{h,0}^m$, the space $V_{h,0}^{m,\circ}$ is selected to be the standard C^0 finite element space with the order $1 \le m \le 3$. The parameter μ is fixed as 10.

Example 1 In this test, we set the domain $\Omega_0 := \{(x, y) \in \mathbb{R}^2 \mid \phi(x, y) < 0\}$ to be a disk (see Fig. 3) with radius $r = 0.7$, that is, $\phi(x, y) = x^2 + y^2 - r^2$. We take the background mesh $\mathcal{T}_h$ that partitions the squared domain $\Omega = (-1, 1)^2$ into triangular elements with the mesh size $h = 1/5, \ldots, 1/40$; see Fig. 3. The exact solution is given as

$$u(x, y) = \sin(2\pi x)\sin(4\pi y).$$

The numerical errors under both the L^2 norm and the energy norm are presented in Table 1. From the results, the optimal convergence rate under $\|\cdot\|_{\mathrm{DG}}$ is observed, which is in the perfect agreement with the theoretical estimate (24) for the 2D case. We point out that the optimal L^2 convergence rates are also numerically detected for all m, even though the bilinear form $a_h(\cdot, \cdot)$ is non-symmetric (cf. Remark 3).

Example 2 The second test is to solve the 2D elliptic problem defined on the flower-like domain [21] (see Fig. 4), where Ω_0 is governed by the level set function $\phi < 0$, where

$$\phi(r, \theta) = r - 0.6 - 0.2\cos(5\theta),$$

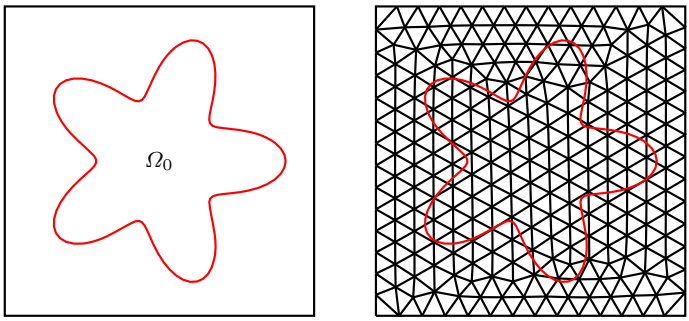

Fig. 4 The curved domain and the partition of Example 2

Table 2 Numerical errors of Example 2

m	h	1/6	1/12	order	1/24	order	1/48	order
1	$\|\boldsymbol{u}-\boldsymbol{u}_h\|_{L^2(\Omega_0)}$	2.555e−1	6.858e−2	1.89	1.792e−2	1.93	3.896e−3	2.22
	$\|\boldsymbol{u}-\boldsymbol{u}_h\|_{\mathrm{DG}}$	4.508e−0	2.100e−0	1.10	9.683e−1	1.11	4.403e−1	1.13
2	$\|\boldsymbol{u}-\boldsymbol{u}_h\|_{L^2(\Omega_0)}$	3.132e−2	2.592e−3	3.59	2.332e−4	3.48	2.902e−5	3.01
	$\|\boldsymbol{u}-\boldsymbol{u}_h\|_{\mathrm{DG}}$	9.998e−1	1.851e−1	2.43	3.646e−2	2.34	8.280e−3	2.13
3	$\|\boldsymbol{u}-\boldsymbol{u}_h\|_{L^2(\Omega_0)}$	2.933e−3	1.169e−4	4.64	6.649e−6	4.13	3.547e−7	4.22
	$\|\boldsymbol{u}-\boldsymbol{u}_h\|_{\mathrm{DG}}$	1.193e−1	1.055e−2	3.50	1.070e−3	3.30	1.100e−4	3.26

with the polar coordinates (r, θ). The exact solution [21] reads

$$u(x, y) = \cos(2\pi x)\cos(2\pi y) + \sin(2\pi x)\sin(2\pi y).$$

We solve (17) on a series of triangular meshes ($h = 1/6, 1/12, 1/24, 1/48$) on the domain $\Omega = (-1, 1)^2$ (see Fig. 4). The errors under two error measurements are gathered in Table 2. For such a curved domain, our method also demonstrates that the errors $\|u - u_h\|_{L^2(\Omega)}$ and $\|u - u_h\|_{\mathrm{DG}}$ approach zero at the optimal rates $O(h^{m+1})$ and $O(h^m)$, respectively, which are well consistent with the results in Theorem 2.

Example 3 In this test, we solve a 3D elliptic problem defined in a spherical domain Ω_0 (see Fig. 5), whose corresponding level set function reads

$$\phi(x, y, z) = (x - 0.5)^2 + (y - 0.5)^2 + (z - 0.5)^2 - r^2,$$

with the radius $r = 0.35$. The exact solution u is chosen as

$$u(x, y, z) = \cos(\pi x)\cos(\pi y)\cos(\pi z).$$

We take a series of tetrahedral meshes, with the mesh size $h = 1/8, 1/16, 1/32, 1/64$, that cover the domain $\Omega = (0, 1)^3$. The numerical results in Table 3 show that the proposed method still has the optimal convergence rates for the errors $\|u - u_h\|_{L^2(\Omega)}$ and $\|u - u_h\|_{\mathrm{DG}}$.

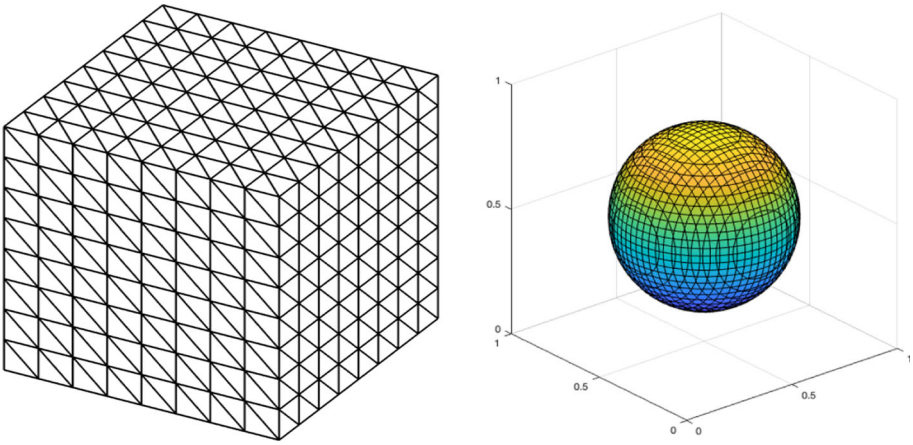

Fig. 5 The spherical domain and the tetrahedral mesh of Example 3

5.2 Convergence Studies for Elliptic Interface Problems

This subsection is devoted to verify the theoretical analysis of the interface-unfitted scheme (29). The spaces $V_{h,0}^{m,\circ}$ and $V_{h,1}^{m,\circ}$ are taken as the C^0 finite element spaces. The parameter η is selected as 10.

Example 4 This test is a 2D benchmark problem on $\Omega = (-1, 1)^2$ that contains a circular interface (see Fig. 6),

$$\phi(x, y) = x^2 + y^2 - r^2,$$

with radius $r = 0.5$. The piecewise coefficient α in (28) and the exact solution are respectively taken to be

$$\alpha = \begin{cases} b, & \phi(x, y) > 0, \\ 1, & \phi(x, y) < 0, \end{cases} \quad u(x, y) = \begin{cases} -\frac{1}{b}\left(\frac{(x^2+y^2)^2}{2} + x^2 + y^2\right), & \phi(x, y) > 0, \\ \sin(2\pi x)\sin(\pi y), & \phi(x, y) < 0, \end{cases}$$

with $b = 10$. We adopt triangular meshes with $h = 1/10, \ldots, 1/80$ and $1 \le m \le 3$. Numerical results are collected in Table 4. We can observe that the proposed unfitted method yields $O(h^{m+1})$and $O(h^m)$ convergence rates for the errors $\|u - u_h\|_{L^2(\Omega)}$ and $|||u - u_h|||_{\mathrm{DG}}$, respectively. This is in accordance with the predicted results in Theorem 5.

Further, we also test the case, by choosing $b = 1000$, that the coefficient has a large jump. The numerical results are shown in Table 5. By comparing the errors in Table 4 with those in Table 5, the robustness of the proposed method is demonstrated for the problem involving a big contrast on the interface.

Example 5 We consider an elliptic interface problem with a star interface [48] (see Fig. 7), where Γ is parametrized with the polar coordinate (r, θ),

$$\phi(r, \theta) = r - \frac{1}{2} - \frac{\sin(5\theta)}{7}.$$

Table 3 Numerical errors of Example 3

m	h	1/8	1/16	order	1/32	order	1/64	order
1	$\|\boldsymbol{u}-\boldsymbol{u}_h\|_{L^2(\Omega_0)}$	9.385e−3	3.119e−3	1.59	9.278e−4	1.93	2.076e−4	2.16
	$\|\boldsymbol{u}-\boldsymbol{u}_h\|_{\mathrm{DG}}$	2.390e−1	1.361e−1	0.81	6.516e−2	1.06	3.031e−2	1.10
2	$\|\boldsymbol{u}-\boldsymbol{u}_h\|_{L^2(\Omega_0)}$	1.459e−3	7.350e−5	4.31	7.536e−6	3.28	2.613e−5	3.06
	$\|\boldsymbol{u}-\boldsymbol{u}_h\|_{\mathrm{DG}}$	5.342e−2	7.891e−3	2.76	1.751e−3	2.17	4.130e−4	2.09
3	$\|\boldsymbol{u}-\boldsymbol{u}_h\|_{L^2(\Omega_0)}$	8.659e−5	3.891e−6	4.47	1.975e−7	4.30	1.067e−8	4.21
	$\|\boldsymbol{u}-\boldsymbol{u}_h\|_{\mathrm{DG}}$	3.286e−3	2.857e−4	3.52	2.928e−5	3.28	3.253e−6	3.17

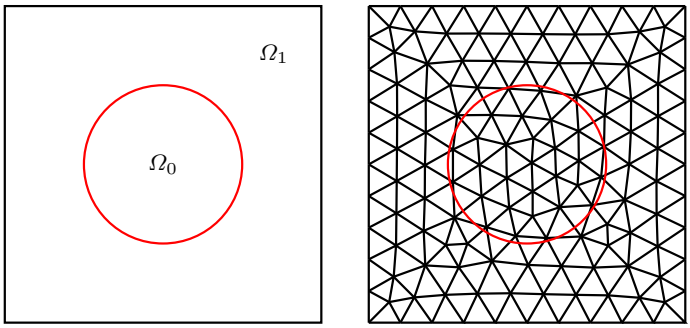

Fig. 6 The interface and the partition of Example 4

Table 4 Numerical errors of Example 4: $b = 10$

m	h	1/10	1/20	order	1/40	order	1/80	order
1	$\|\boldsymbol{u}-\boldsymbol{u}_h\|_{L^2(\Omega_0)}$	2.888e−2	7.250e−3	1.99	1.345e−3	2.43	3.407e−4	1.99
	$\|\boldsymbol{u}-\boldsymbol{u}_h\|_{\mathrm{DG}}$	7.817e−1	3.580e−1	1.12	1.636e−1	1.13	7.968e−2	1.03
2	$\|\boldsymbol{u}-\boldsymbol{u}_h\|_{L^2(\Omega_0)}$	7.379e−4	9.642e−5	2.93	9.308e−6	3.37	1.162e−6	3.00
	$\|\boldsymbol{u}-\boldsymbol{u}_h\|_{\mathrm{DG}}$	4.816e−2	1.178e−2	2.03	2.560e−3	2.20	6.235e−4	2.03
3	$\|\boldsymbol{u}-\boldsymbol{u}_h\|_{L^2(\Omega_0)}$	6.590e−5	3.633e−6	4.18	1.752e−7	4.37	1.025e−8	4.10
	$\|\boldsymbol{u}-\boldsymbol{u}_h\|_{\mathrm{DG}}$	4.511e−3	4.946e−4	3.19	4.666e−5	3.39	5.399e−6	3.11

Table 5 Numerical errors of Example 4 with a large jump: $b = 1000$

m	h	1/8	1/16	order	1/32	order	1/64	order
1	$\|\boldsymbol{u}-\boldsymbol{u}_h\|_{L^2(\Omega_0)}$	3.080e−3	7.615e−3	2.01	1.279e−3	2.57	2.928e−4	2.13
	$\|\boldsymbol{u}-\boldsymbol{u}_h\|_{\mathrm{DG}}$	7.371e−1	3.248e−1	1.18	1.444e−1	1.17	6.981e−2	1.05
2	$\|\boldsymbol{u}-\boldsymbol{u}_h\|_{L^2(\Omega_0)}$	7.062e−4	8.515e−5	3.05	8.565e−6	3.31	1.027e−6	3.06
	$\|\boldsymbol{u}-\boldsymbol{u}_h\|_{\mathrm{DG}}$	4.765e−2	1.153e−2	2.05	2.531e−3	2.18	6.163e−4	2.03
3	$\|\boldsymbol{u}-\boldsymbol{u}_h\|_{L^2(\Omega_0)}$	5.942e−5	3.226e−6	4.20	1.461e−7	4.46	9.068e−9	4.01
	$\|\boldsymbol{u}-\boldsymbol{u}_h\|_{\mathrm{DG}}$	4.502e−3	4.947e−4	3.18	4.685e−5	3.40	5.460e−6	3.10

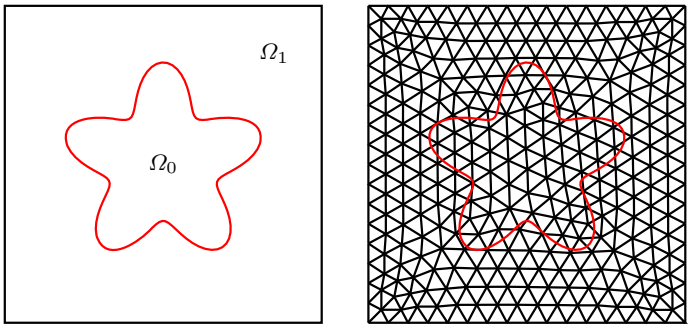

Fig. 7 The interface and the partition of Example 5

Table 6 Numerical errors of Example 5

m	h	1/8	1/16	order	1/32	order	1/64	order
1	$\|\boldsymbol{u}-\boldsymbol{u}_h\|_{L^2(\Omega_0)}$	1.958e−2	2.253e−3	3.12	4.607e−4	2.29	1.055e−4	2.12
	$\|\boldsymbol{u}-\boldsymbol{u}_h\|_{\mathrm{DG}}$	4.876e−1	1.029e−1	2.21	4.486e−2	1.13	2.216e−2	1.07
2	$\|\boldsymbol{u}-\boldsymbol{u}_h\|_{L^2(\Omega_0)}$	2.813e−3	1.399e−4	4.33	1.489e−5	3.23	1.583e−6	3.23
	$\|\boldsymbol{u}-\boldsymbol{u}_h\|_{\mathrm{DG}}$	3.137e−2	2.735e−2	3.52	5.205e−4	2.39	1.163e−4	2.16
3	$\|\boldsymbol{u}-\boldsymbol{u}_h\|_{L^2(\Omega_0)}$	2.501e−4	4.667e−6	5.72	7.156e−6	4.29	3.973e−8	4.17
	$\|\boldsymbol{u}-\boldsymbol{u}_h\|_{\mathrm{DG}}$	1.793e−2	9.166e−4	4.29	8.866e−5	3.37	9.000e−6	3.29

The domain is $\Omega = (-1, 1)^2$. The coefficient α and the exact solution are selected to be

$$\alpha = \begin{cases} 10, & \phi(r,\theta) > 0, \\ 1, & \phi(r,\theta) < 0, \end{cases} \quad u(r,\theta) = \begin{cases} 0.1r^2 - 0.01\ln(2r), & \phi(r,\theta) > 0, \\ e^{r^2}, & \phi(r,\theta) < 0, \end{cases}$$

respectively. We display the numerical results in Table 6. Similar as the previous example, the optimal convergence rates for the errors under the L^2 norm and the energy norm can be still observed.

Example 6 In the last example, we consider the elliptic interface problem (28) in three dimensions with the coefficient $\alpha = 1$. The domain is the unit cube $\Omega = (0, 1)^3$ and the interface is a smooth molecular surface of two atoms (see Fig. 8), which is given by the level set function [38, 46],

$$\begin{aligned} \phi(x, y, z) = &\big((2.5(x-0.5))^2 + (4(y-0.5))^2 + (2.5(z-0.5))^2 + 0.6\big)^2 \\ &-3.5(4(y-0.5))^2 - 0.6. \end{aligned}$$

The exact solution takes the form

$$u(x, y, z) = \begin{cases} e^{2(x+y+z)}, & \phi(x, y, z) > 0, \\ \sin(2\pi x)\sin(2\pi y)\sin(2\pi z), & \phi(x, y, z) < 0. \end{cases}$$

The initial mesh $\mathcal{T}_h$ is taken as a tetrahedral with $h = 1/4$, and we solve the interface problem on a series of successively refined meshes (see Fig. 5). The convergence histories with $1 \le m \le 3$ are reported in Table 7, which show that both errors $\|u - u_h\|_{L^2(\Omega)}$ and

Table 7 Numerical errors of the Example 6

m	h	1/4	1/8	order	1/16	order	1/32	order
1	$\|\boldsymbol{u}-\boldsymbol{u}_h\|_{L^2(\Omega_0)}$	1.651e−0	6.115e−1	1.52	1.537e−1	1.99	3.501e−2	2.13
	$\|\boldsymbol{u}-\boldsymbol{u}_h\|_{\mathrm{DG}}$	3.779e+1	1.992e+1	1.08	7.688e−0	1.22	3.679e−0	1.06
2	$\|\boldsymbol{u}-\boldsymbol{u}_h\|_{L^2(\Omega_0)}$	2.278e−1	1.906e−2	3.57	2.223e−3	3.10	2.494e−4	3.15
	$\|\boldsymbol{u}-\boldsymbol{u}_h\|_{\mathrm{DG}}$	4.603e−0	8.356e−1	2.46	1.636e−1	2.37	3.817e−2	2.10
3	$\|\boldsymbol{u}-\boldsymbol{u}_h\|_{L^2(\Omega_0)}$	8.736e−2	5.624e−3	3.95	2.738e−4	4.36	1.419e−5	4.26
	$\|\boldsymbol{u}-\boldsymbol{u}_h\|_{\mathrm{DG}}$	1.022e−0	8.752e−2	3.09	8.406e−3	3.38	9.275e−4	3.17

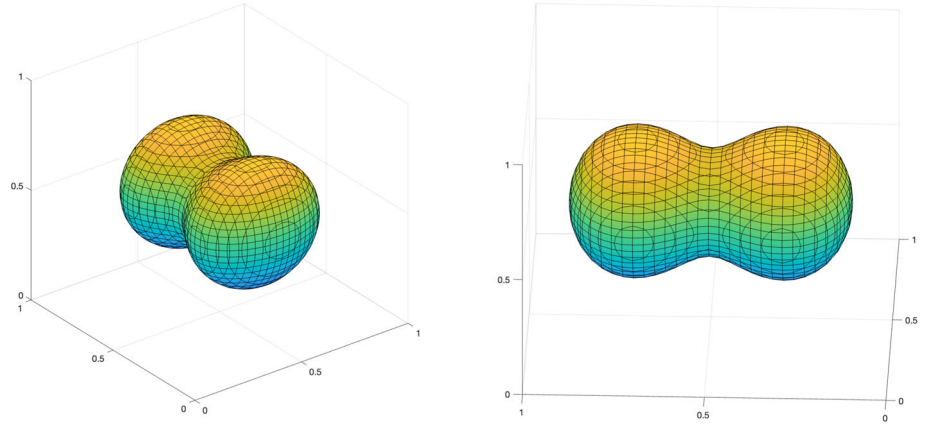

Fig. 8 The interface of Example 6

$|||u-u_h|||_{\mathrm{DG}}$ decrease to zero at their optimal convergence rates. This observation again validates the theoretical predictions in Theorem 5.

5.3 Condition Number Studies

We compute the condition numbers of the stiffness matrices coming from the elliptic problem on the curved domain and the elliptic interface problem, respectively. Theorems 3 and 6 claim that for both problems, the condition numbers will grow at the speed $O(h^{-2})$. In Fig. 9, we show the condition numbers of the stiffness matrices corresponding to Example 1 and Example 4, respectively. The numerically detected results confirm our theoretical rates. The condition number seems to be relatively large especially for the high-order accuracy. There may be two underlying factors that affect the condition number. The first is the penalty parameter μ. From the bilinear forms, the condition number is nearly linearly dependent on μ. Hence, a small value of μ is recommended (we fix $\mu = 1$ in the numerical tests), and we note that our method is stable for any $\mu > 0$. The second factor is the local extension of the polynomial. The extension is similar to the extrapolation of polynomials. The value of the extrapolation grows fast outside the data domain, which may lead to a large condition number. To overcome this difficulty we may require some stable projection techniques, which is a future work for us.

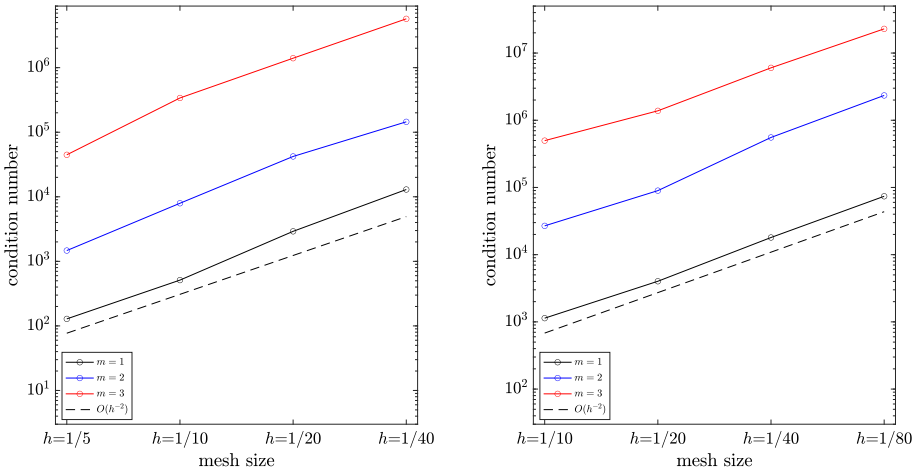

Fig. 9 Condition numbers of the final linear systems of Example 1 (left) and Example 4 (right)

6 Conclusion

We have developed an unfitted finite element method of arbitrary order for curved domain elliptic problems and elliptic interface problems. The degrees of freedom of the used approximation spaces are totally located in the elements that are not cut by the domain boundary/interface. In the non-symmetric interior penalty schemes, the boundary/jump conditions are weakly imposed by Nitsche's method. The stability near the boundary or the interface does not require any stabilization technique or any constraint on the mesh, which means that our method allows the curved boundary/interface to intersect the mesh arbitrarily. The method is of optimal convergence order under the energy norm. In addition, we have given upper bounds of the condition numbers for final linear systems. A series of numerical examples in two and three dimensions demonstrate the good performance of our method.

Acknowledgements The authors would like to thank the anonymous referee sincerely for the constructive comments that improve the quality of this paper. This work was supported by National Natural Science Foundation of China (12201442, 12171340, 11971041) and National Key R&D Program of China (2020YFA0714000).

Funding The authors declare that they have no funding.

Data Availability Enquiries about data availability should be directed to the authors.

Declarations

Conflict of interest The authors have not disclosed any competing interests.

References

1. Adams, R.A., Fournier, J.J.F.: Sobolev Spaces, Pure and Applied Mathematics (Amsterdam), vol. 140, 2nd edn. Elsevier/Academic Press, Amsterdam (2003)

2. Areias, P.M.A., Belytschko, T.: Letter to the editor: A comment on the article: "A finite element method for the simulation of strong and weak discontinuities in solid mechanics" [Comput. Methods Appl. Mech. Engrg. **193** (2004)(33-35), 3523–3540; mr2075053] by Hansbo, A., Hansbo, P. Comput. Methods Appl. Mech. Engrg. **195** (2006)(9-12), 1275–1276
3. Ayuso de Dios, B., Brezzi, F., Havle, O., Marini, L.D.: L^2-estimates for the DG IIPG-0 scheme. Numer. Methods Partial Diff. Equ. **28**(5), 1440–1465 (2012)
4. Babuška, I., Banerjee, U.: Stable generalized finite element method (SGFEM). Comput. Methods Appl. Mech. Eng. **201**(204), 91–111 (2012)
5. Badia, S., Verdugo, F., Martín, A.: The aggregated unfitted finite element method for elliptic problems. Comput. Methods Appl. Mech. Eng. **336**, 533–553 (2018)
6. Belytschko, T., Gracie, R., Ventura, G.: A review of extended/generalized finite element methods for material modeling. Modelling Simul. Mater. Sci. Eng. **17**(4), 043001 (2009)
7. Bordas, S.P.A., Burman, E., Larson, M.G., Olshanskii, M.A. (eds.), Geometrically unfitted finite element methods and applications. In: Lecture Notes in Computational Science and Engineering. Springer, Cham, 2017, Held (2016)
8. Brenner, S.C., Scott, L.R.: The Mathematical Theory of Finite Element Methods, Texts in Applied Mathematics, vol. 15, 3rd edn. Springer, New York (2008)
9. Burman, E.: Ghost penalty. C. R. Math. Acad. Sci. Paris **348**(21–22), 1217–1220 (2010)
10. Burman, E., Cicuttin, M., Delay, G., Ern, A.: An unfitted hybrid high-order method with cell agglomeration for elliptic interface problems. SIAM J. Sci. Comput. **43**(2), A859–A882 (2021)
11. Burman, E., Claus, S., Hansbo, P., Larson, M.G., Massing, A.: CutFEM: discretizing geometry and partial differential equations. Int. J. Numer. Methods Eng. **104**(7), 472–501 (2015)
12. Burman, E., Hansbo, P.: Fictitious domain finite element methods using cut elements: II. A stabilized Nitsche method. Appl. Numer. Math. **62**(4), 328–341 (2012)
13. Burman, E., Hansbo, P.: Fictitious domain methods using cut elements: III. A stabilized Nitsche method for Stokes' problem. ESAIM Math. Model. Numer. Anal. **48**(3), 859–874 (2014)
14. Burman, E., Hansbo, P., Larson, M.G., Massing, A.: A stable cut finite element method for partial differential equations on surfaces: the Helmholtz-Beltrami operator. Comput. Methods Appl. Mech. Eng. **362**, 112803, 21 (2020)
15. Cui, T., Leng, W., Liu, H., Zhang, L., Zheng, W.: High-order numerical quadratures in a tetrahedron with an implicitly defined curved interface. ACM Trans. Math. Softw. (2019), **46**(1), 1–18 (2019)
16. de Prenter, F., Lehrenfeld, C., Massing, A.: A note on the stability parameter in Nitsche's method for unfitted boundary value problems. Comput. Math. Appl. **75**(12), 4322–4336 (2018)
17. Dolejší, V., Havle, O.: The L^2-optimality of the IIPG method for odd degrees of polynomial approximation in 1D. J. Sci. Comput. **42**(1), 122–143 (2010)
18. Fries, T.-P., Belytschko, T.: The extended/generalized finite element method: an overview of the method and its applications. Int. J. Numer. Methods Eng. **84**(3), 253–304 (2010)
19. Girault, V., Raviart, P.-A.: Finite element methods for Navier-Stokes equations. In: Springer-Verlag, Berlin, 1986
20. Gürkan, C., Massing, A.: A stabilized cut discontinuous Galerkin framework for elliptic boundary value and interface problems. Comput. Methods Appl. Mech. Eng. **348**, 466–499 (2019)
21. Gürkan, C., Massing, A.: A stabilized cut discontinuous Galerkin framework for elliptic boundary value and interface problems. Comput. Methods Appl. Mech. Eng. **348**, 466–499 (2019)
22. Gürkan, C., Sticko, S., Massing, A.: Stabilized cut discontinuous Galerkin methods for advection-reaction problems. SIAM J. Sci. Comput. **42**(5), A2620–A2654 (2020)
23. Guzmán, J., Olshanskii, M.: Inf-sup stability of geometrically unfitted Stokes finite elements. Math. Comp. **87**(313), 2091–2112 (2018)
24. Guzmán, J., Rivière, B.: Sub-optimal convergence of non-symmetric discontinuous Galerkin methods for odd polynomial approximations. J. Sci. Comput. **40**(1–3), 273–280 (2009)
25. Han, Y., Chen, H., Wang, X., Xie, X.: EXtended HDG methods for second order elliptic interface problems. J. Sci. Comput. **84**(1), 29 (2020)
26. Hansbo, A., Hansbo, P.: An unfitted finite element method, based on Nitsche's method, for elliptic interface problems. Comput. Methods Appl. Mech. Eng. **191**(47–48), 5537–5552 (2002)
27. Hansbo, P., Larson, M.G.: Discontinuous Galerkin methods for incompressible and nearly incompressible elasticity by Nitsche's method. Comput. Methods Appl. Mech. Eng. **191**(17–18), 1895–1908 (2002)
28. Hansbo, P., Larson, M.G., Zahedi, S.: A cut finite element method for a Stokes interface problem. Appl. Numer. Math. **85**, 90–114 (2014)
29. Huang, P., Wu, H., Xiao, Y.: An unfitted interface penalty finite element method for elliptic interface problems. Comput. Methods Appl. Mech. Eng. **323**, 439–460 (2017)

30. Johansson, A., Larson, M.G.: A high order discontinuous Galerkin Nitsche method for elliptic problems with fictitious boundary. Numer. Math. **123**(4), 607–628 (2013)
31. Kellogg, R.B.: Higher order singularities for interface problems, The mathematical foundations of the finite element method with applications to partial differential equations. In: Proc. Sympos., Univ. Maryland, Baltimore, Md., pp. 589–602 (1972). MR 0433926
32. Kellogg, R.B., Osborn, J.E.: A regularity result for the Stokes problem in a convex polygon. J. Funct. Anal. **21**(4), 397–431 (1976)
33. Kramer, R., Bochev, P., Siefert, C., Voth, T.: An extended finite element method with algebraic constraints (XFEM-AC) for problems with weak discontinuities. Comput. Methods Appl. Mech. Eng. **266**, 70–80 (2013)
34. Larson, M.G., Niklasson, A.J.: Analysis of a family of discontinuous Galerkin methods for elliptic problems: the one dimensional case. Numer. Math. **99**(1), 113–130 (2004)
35. Lehrenfeld, C.: High order unfitted finite element methods on level set domains using isoparametric mappings. Comput. Methods Appl. Mech. Eng. **300**, 716–733 (2016)
36. Lehrenfeld, C., Reusken, A.: Analysis of a high-order unfitted finite element method for elliptic interface problems. IMA J. Numer. Anal. **38**(3), 1351–1387 (2018)
37. Li, K., Atallah, N.-M., Main, G.-A., Scovazzi, G.: The shifted interface method: a flexible approach to embedded interface computations. Int. J. Numer. Methods Eng. **121**(3), 492–518 (2020)
38. Li, R., Yang, F.: A discontinuous Galerkin method by patch reconstruction for elliptic interface problem on unfitted mesh. SIAM J. Sci. Comput. **42**(2), A1428–A1457 (2020)
39. Li, Z.: The immersed interface method using a finite element formulation. Appl. Numer. Math. **27**(3), 253–267 (1998)
40. Lin, T., Lin, Y., Zhang, X.: Partially penalized immersed finite element methods for elliptic interface problems. SIAM J. Numer. Anal. **53**(2), 1121–1144 (2015)
41. Main, A., Scovazzi, G.: The shifted boundary method for embedded domain computations. Part I: poisson and Stokes problems. J. Comput. Phys. **372**, 972–995 (2018)
42. Massing, A., Larson, M.G., Logg, A., Rognes, M.E.: A stabilized Nitsche fictitious domain method for the Stokes problem. J. Sci. Comput. **61**(3), 604–628 (2014)
43. Neiva, E., Badia, S.: Robust and scalable *h*-adaptive aggregated unfitted finite elements for interface elliptic problems. Comput. Methods Appl. Mech. Eng. **380**, 26 (2021)
44. Saye, R.I.: High-order quadrature methods for implicitly defined surfaces and volumes in hyperrectangles. SIAM J. Sci. Comput. **37**(2), A993–A1019 (2015)
45. Strouboulis, T., Babuška, I., Copps, K.: The design and analysis of the generalized finite element method. Comput. Methods Appl. Mech. Eng. **181**(1–3), 43–69 (2000)
46. Wei, Z., Li, C., Zhao, S.: A spatially second order alternating direction implicit (ADI) method for solving three dimensional parabolic interface problems. Comput. Math. Appl. **75**(6), 2173–2192 (2018)
47. Wu, H., Xiao, Y.: An unfitted *hp*-interface penalty finite element method for elliptic interface problems. J. Comput. Math. **37**(3), 316–339 (2019)
48. Zhou, Y.C., Wei, G.W.: On the fictitious-domain and interpolation formulations of the matched interface and boundary (MIB) method. J. Comput. Phys. **219**(1), 228–246 (2006)